

**THE UTILIZATION OF SMALL DIAMETER
TIMBERS IN PULTRUDED LONG
STRAND COMPOSITES**

By

ZACHARY SCOTT RININGER

A thesis submitted in partial fulfillment of
the requirements for the degree of

MASTER OF SCIENCE IN CIVIL ENGINEERING

WASHINGTON STATE UNIVERSITY

Department of Civil and Environmental Engineering

AUGUST 2008

To the Faculty of Washington State University:

The members of the Committee appointed to examine the thesis of ZACHARY SCOTT
RININGER find it satisfactory and recommend that it be accepted.

Co-Chair

Co-Chair

Acknowledgement

I would like to start by thanking my major professors and co-chairs Karl Englund and Michael Wolcott, also the final member of my committee Vikram Yadama. Without their assistance none of this would be possible. Thank you also to the USDA Wood Utilization Research Program for funding this research.

Thank you to the numerous companies that contributed to this research: Weyerhaeuser iLevel for their assistance in generating strands. Potlatch Corporation for providing veneer. Arclin for providing oriented strand board PF resin. Hexion Specialty Chemicals for providing veneer PF resin. YLA inc. for providing carbon fiber. The assistance that these companies provided is greatly appreciated.

Thank you to the entire civil engineering department and wood materials and engineering laboratory (WMEL) staff and faculty for all of their support and assistance. Enough cannot be said of the technical assistance and guidance of Brent Olsen, Bob Duncan, and Scott Lewis, thank you all. Fellow graduate students and WMEL laboratory aides: Tony Cameron, Steve Michaels, Yi Wang, Stephanie Pitts, and Zachary Andrews thank you for all of your help in the laboratory.

Finally to my family: Kent, Lisa, Charley, Ben, Sam, Nalani, friends in Pullman, and friends in Seward thank you so much for all the support and guidance. There is no question that without you I would have never been able to make it this point.

THE UTILIZATION OF SMALL DIAMETER TIMBERS IN PULTRUDED LONG
STRAND COMPOSITES

Abstract

By Zachary Scott Rininger, M.S.
Washington State University
August 2008

Chairs: Karl Englund & Michael P. Wolcott

The feasibility of utilizing a pultrusion process to produce long strand composites was modeled using solid-mechanics, and the use of small diameter timber as a material source for strand based composites was analyzed. The success of a strand composite pultrusion process is dependent on the tensile capacity of the strand composite exceeding the accumulated pulling force developed in the pultrusion die.

Three under-utilized species of small diameter timber commonly found in the Pacific Northwest were characterized for their strand quality and composite properties. Physical attributes such as; strand dimensions, grain angle, and strand orientation within a mat were characterized. Ultimate tensile strength and tension modulus of both individual strands and prototype strand composites at a range of densities were also characterized. Other properties that were also characterized were variation in density along a panel and the percentage of usable strands yielded from the stranding process.

The pulling force developed in the pultrusion die was described using a combination of consolidation and frictional forces along with the geometry of the pultrusion die. Proper modeling of these forces is crucial in the success of a wood strand pultrusion operation.

Mat consolidation stresses were predicted using models by Dai & Steiner (1993) and Zhou & Dai (2008) that employ theories of strand bending within a strand mat and strand mat compression. Mat relaxation stresses were modeled using a Maxwell model that describes the viscoelastic response of a strand mat during pressing. Frictional coefficients were tested and described by utilizing veneers, uni-axial compression, and sliding friction response. A mechanics of materials approach was employed to derive an equation to describe the summation of frictional and normal forces in the pultrusion die. The equations for frictional and normal forces were set up as integrals to allow for the accumulated pulling force developed along the length of the pultrusion die to be determined. A pultrusion process was developed to test the technical feasibility. This pultrusion process was based on a previously successful pultrusion process for fibrous mats (Englund, 2001). Mechanical limitations of the pultrusion process did not permit validation of pulling force model.

TABLE OF CONTENTS

Acknowledgement	iii
Abstract	iv
Table of Contents	vi
List of Figures	ix
CHAPTER 1 : Introduction	1
Abstract	1
Introduction	1
Project Objectives	5
References	7
CHAPTER 2 : Long Strand Composites Utilizing Small Diameter Timbers	8
Abstract	8
Introduction	8
Project Objectives	11
Methods & Materials	11
Strand Processing	11
Strand Physical Attribute Measuring	12
Strand Tensile Testing	13
Unidirectional Stand Composite Manufacture	13
Unidirectional Stand Composite Testing	14
Statistical Analysis	15
Results & Discussion	16
Strand Geometry	16

Grain Angle.....	17
Strand tensile properties.....	19
Processing data.....	21
Composite tensile properties.....	22
Conclusions	24
References.....	25
CHAPTER 3 : Feasibility of Producing Pultruded Long Strand Composites	28
Abstract.....	28
Introduction.....	28
Compression of panel products.....	30
Consolidation Stress.....	32
Relaxation Stress.....	33
Friction	33
Objectives	34
Model Development	35
Modeling of Pulling Force	35
Modeling of Consolidation Stresses	38
Modeling of Relaxation Stresses.....	41
Methods & Materials	42
Experimental Data for Model Development.....	42
Consolidation Model – Experimental Methods	42
Friction	43
Density Adjustment	44

Pultrusion	45
Results & Discussion	46
Consolidation Stress.....	46
Relaxation Stress.....	49
Friction Coefficient.....	50
Pulling Force Model	51
Optimization of Entrance Angle	54
Friction Sensitivity.....	55
Density Variation	56
Pultrusion of Wood Strand Composites.....	57
Conclusion	58
References.....	59
CHAPTER 4 : Project Summary & Conclusions.....	62
APPENDIX A – GLM Procedure & Duncan Test For Strand Dimensions	1
APPENDIX B - Cumulative Frequency Plots of Strand Dimensions	6
APPENDIX C - GLM Procedure & Duncan Test For Grain Angle.....	8
APPENDIX D - GLM Procedure & Duncan Test For Strand Tensile Properties.....	10
APPENDIX E - Strand Composite Tensile Properties & Density Relationships.....	13
APPENDIX F - Accumulated Pulling Force Along Length of Pultrusion Die	14

LIST OF FIGURES

Figure 2.1- Grain angle measurement.....	12
Figure 2.2 - Cumulative plot for strand width	17
Figure 2.3 - Cumulative plot for slenderness ratio	17
Figure 2.4 -Cumulative plot of grain angle.....	18
Figure 2.5- Cumulative plot of ultimate tensile strength	19
Figure 2.6- Cumulative plot of tension modulus	20
Figure 2.7- Comparison of ultimate tensile strength values with values form ASTM Standard D2555	21
Figure 2.8 - Percentage of accepted strands from stranding process	22
Figure 2.9 -Composite ultimate tension modulus with density	23
Figure 2.10- Composite ultimate tensile strength with density	24
Figure 3.1 - Pultrusion process overview	29
Figure 3.2 -Friction & normal forces in the pultrusion die.....	30
Figure 3.3- Compaction pressure during flat pressing (Wolcott, 1990)	31
Figure 3.4 - Overview development in pultrusion die	35
Figure 3.5 - Test procedure for determining coefficient of friction (Englund, 2001)	44
Figure 3.6 - Predicted & experimental consolidation stress for grand fir.....	48
Figure 3.7 - Predicted & experimental consolidation stress for lodgepole pine.....	48
Figure 3.8 - Predicted & experimental consolidation stress for ponderosa pine	48
Figure 3.9 - Relaxation stress for ponderosa pine mat compressed to 560 kg/m^3	50
Figure 3.10 -Relaxation stress for grand fir strand mat compressed to 800 kg/m^3	50
Figure 3.11 - Dynamic & static frictional coefficients with temperature.....	51

Figure 3.12 - Comparison of pulling force and ultimate tensile strength for ponderosa pine.....	52
Figure 3.13 - Comparison of pulling force and ultimate tensile strength for lodgepole pine	52
Figure 3.14 -Comparison of pulling force and ultimate tensile strength for grand fir.....	53
Figure 3.15 - Accumulated pulling force for ponderosa pine.....	54
Figure 3.16- Pulling force in entrance section with varying entrance angles.....	55
Figure 3.17- Density variation in prototype panels	56

LIST OF TABLES

Table 2-1- Average strand dimensions	16
Table 2-2- Strand tensile properties	19
Table 2-3 - Average tensile properties of composites	23
Table 3-1 - Parameters for compression stress modeling	47
Table 3-2 - Relaxation stress model parameters	49
Table 3-3 - Calculated pulling force	51
Table 3-4- Pulling forces for extreme friction coefficients	55

CHAPTER 1 : INTRODUCTION

ABSTRACT

The feasibility of utilizing a pultrusion process to produce long strand composites was modeled using solid-mechanics, and the use of small diameter timber as a material source for strand based composites was analyzed. The key factors that will decide whether or not a particular formulation of resin and strands will be suitable for a pultrusion process is the tensile capacity of the wood strand mat during processing and the pulling load developed during processing. The following research characterizes strands from three species of small diameter timbers, models the consolidation behavior of the strands in a uni-directional strand mat, and models the predicted pulling force developed within a pultrusion die using wood strand mats at a range of densities. The goal of this chapter is to introduce concepts with relevance to this project, the second chapter will characterize wood strand and wood strand mat properties for the pultrusion process, the third chapter will model pulling force developed in the system, and the forth chapter will review the conclusions from this research.

INTRODUCTION

In order for the wood composite industry to continue to grow, their efforts need to be concentrated on creative ways to better utilize wood. One way this can be accomplished is to utilize non-traditional processing methods to accommodate the use of wood timbers,

strands and particles. This is the case with such processes as extrusion and injection molding. Extrusion is a continuous process where particulate material is fed into a heated die using a screw driven process (Tadmor, 1937). Injection molding is a batch process where heated material is fed into a cold form die using a screw and/or plunger process (Tadmor, 1937). Another process that has recently been introduced into wood composite research is pultrusion. Pultrusion is a process where continuous fibers are coated in resin and pulled through a stationary die (Barbero, 1999). Previous research found that a pultrusion process could be used to produce a fiber board product using continuous fibrous mats (Englund, 2001). The work suggested that the same pultrusion process could be used to produce oriented strand lumber (OSL) using a similar pultrusion process.

There are many advantages to using a pultrusion process. By pulling the composite through the die rather than using a screw-driven process to push the composite through the die allows the use of larger particles such as strands or fibers. The use of larger fibers generally correlates to higher strength properties. The low mechanical properties of extruded wood plastic composites is one of the major disadvantages of using wood plastic composites as a structural material. Similar to extrusion, a variety of profiles can be formed during the pultrusion process. By changing the geometry of the composite the strength can be maximized with less material to create a more effective composite. The use of less material also will allow for energy to produce the composite. Current processes for producing OSL products lack this capability and use large amounts of energy.

As early as the 1950s pultrusion manufacturing has been used to produce products for electrical applications. Pultrusion has been used to make products ranging from fishing rods to covers on electrical railways to animal feeding troughs (Meyer, 1985). A typical thermoset pultrusion process starts with a continuous fiber roving and/or mat being dispensed from racks and guided into the position of the cross section of the composite. The fiber roving then goes into an injection chamber where thermoset resin is applied. Next the material enters a heated die which has the shape of the desired cross section. The heat from the die cures the resin giving the composite its final cross sectional shape. The composite is pulled through the die with a pulling mechanism and cut into the desired lengths by a flying cut-off saw. Traditional pultrusion manufacturing has been used with continuous fibers and high amounts of thermoset resin. Usually glass fibers and polyester or vinyl ester resins are used because of their low cost (Barbero, 1999).

The concept of pultruding wood composites provides new challenges that are not commonly seen in a pultrusion operation. In a traditional pultrusion operation a fluid based model is used to analyze the material behavior. Traditional pultrusion research focuses on cure kinetics and not pulling forces due to the low viscosity resins and high strength composites. With wood strands a solid mechanics based model needs to be implemented. In wood-strand pultrusion the heated die is used to consolidate the strand mat to its final thickness and cure the resin. In this way the pultrusion die acts similar to conventional wood panel pressing techniques. The first section of the pultrusion die is the tapered entrance, which emulates a press closing step where the strands are

consolidated to a final thickness. The second section is the constant geometry section, where the composite is held constant until the thermoset resin cures similar to a fixed platen dwell time.

The high compressive stress accumulated during consolidation of the wood strands throughout the pultrusion die will result in large tensile loads to the composite. To withstand the tensile load, an optimization of tensile properties in the wood strand mat is essential. Modeling the amount of pulling force required to convey the composite through the die is crucial to understanding and reducing the pulling force in a strand pultrusion process.

The current goal in forest management in the Northwest is to restore the forest ecosystem through restoration and management. Studies show that ecosystem restoration programs may greatly improve forest health by reducing the density of forests, along with reducing the risk of forest fires (Fielder et al, 1999). The USDA estimates that over 56 million acres of forest is in need of varying degrees of restoration (Stewart et al, 2004). A by-product of forest restoration will be the harvest of many small diameter timbers that have very little commercial value. One study estimates that 20% to 30% of the trees harvested during forest restoration will have a diameter of 13 to 25 centimeters (LeVan-Green & Livingston, 2001). By utilizing small diameter timbers to produce a value added product such as a pultruded wood strand composite could increase the feasibility of harvesting small diameter timbers and create a new industry in rural areas.

The following research determines the feasibility of creating a long strand composite that utilizes small diameter timbers in a pultrusion process. Prototype unidirectional composites were manufactured from strands derived from small diameter timbers utilizing flat pressing techniques. These composites were tested for mechanical properties and the compression data that was collected during pressing was used to build a model for predicting the pulling force developed in a pultrusion die. The pulling force and the ultimate tensile strength of the prototype composites were then compared with respect to density to determine a feasible range of densities for a wood strand pultrusion process. A pultrusion process was then developed to attempt to verify the pulling force model predictions.

PROJECT OBJECTIVES

The use of wood strands in a pultrusion manufacturing process is a new concept and very little research has been done in this area. Within the following project the overall goal is to determine the technical feasibility of pultruding a unidirectional wood strand composite made from small diameter timbers. Strand quality and identifying the processing mechanisms and parameters associated with pultruding wood strand composites will need to be determined. The specific objectives of this project are as follows:

- Summarize strand properties produced from small diameter timbers to determine stand properties ideal for producing a pultruded long strand composite made from small diameter timbers.

- Summarize prototype panel properties produced from small diameter timbers using flat pressing techniques to determine panel properties ideal for producing a pultruded long strand composite made from small diameter timbers.
- Develop a pulling force model for uni-directional strand based composites upon the consolidation behavior exhibited in prototype panels.
- Design and construct a pultrusion process for use with long strand composites made from small diameter timbers.

Determining of strand and strand composite properties that will produce ideal strand composites is developed in Chapter 1. Strand properties from small diameter timbers of three species were measured and calculated. Strand properties included strand dimensions, specific gravity, grain angle, tension modulus, ultimate tensile strength, and the percentage of usable strands produced from the stranding process. Statistical analyzes were preformed to determine the significance of species on strand dimensions, strand grain angle and strand tensile properties. Statistical analyzes were also preformed to determine the significance of species and density on strand composite properties.

The development of a solid based model to predict the pulling force developed in the pultrusion die is the focus of Chapter 2. The pulling force model is then compared to ultimate tensile strength of strand composites from Chapter 1 to determine the technical feasibility of a pultrusion process for varying densities and species. The pulling force model is also used to determine the influence of entrance taper in the pultrusion die, the sensitivity of friction, and the influence of density variation on the pultrusion process.

REFERENCES

- Barbero, Ever J. 1999. *Introduction to composite materials design*. New York, NY: Taylor & Francis Group.
- Englund, Karl. 2001. "Consolidation and friction mechanisms of wood composites and their influence on pultrusion processing." Washington State University.
- Fielder, Carl E, Charles E Keegan, Daniel P Wichman, and Stephen F Arno. 1999. "Product and economic implications of ecological restoration." *Forest Products Journal* 49:19-23.
- LeVan-Green, Susan L, and Jean M Livingston. 2001. "Value-added uses for small-diameter trees." *Journal of Forestry* 99:25-26.
- Meyer, Raymond. 1985. *Handbook of pultrusion technology*. New York, NY: Chapman and Hall.
- Stewart, Hayden G, Keith A Blatner, Francis G Wagner, and Charles E Keegan. 2004. "Risk and feasibility of processing small-diameter material in the U.S. West Part I: Structural lumber." *Forest Products Journal* 54:97-103.
- Tadmor, Zehez. 1937. *Principals of Polymer Processing*. 2nd ed. Hoboken, NJ: Wiley-Inerscience.

CHAPTER 2 : LONG STRAND COMPOSITITES UTILIZING SMALL DIAMETER TIMBERS

ABSTRACT

The success of a wood strand pultrusion operation is largely dependent on the tensile capacity of the wood strand composite during processing. For this reason, an understanding of mat and strand properties that influence the tensile capacity of a strand composite must be properly characterized. Three under-utilized species of small diameter timbers commonly found in the Pacific Northwest were characterized for their strand and mat properties. Physical attributes such as; strand dimensions, grain angle, and strand orientation within a mat were characterized. Ultimate tensile strength and tension modulus of both individual strands and prototype strand composites at a range of densities were also characterized. Strand dimensions, tensile properties, and grain angles all showed significant differences between species. Strand composite panels showed significant differences between species and density.

INTRODUCTION

The success of any strand composite depends on mechanical properties of the composite. This is especially true for a pultruded strand composite where the ability to produce a composite is dependent on the tensile capacity of the composite. At any point throughout the pultrusion die the strand composites tensile strength must exceed the accumulated

pulling force. Therefore maximizing the tensile capacity of the strand mat is of the utmost importance. Fortunately increasing mechanical properties of strand composites has been a key focus of strand composite research for the last 50 years.

Post (1958) and Suchsland (1968) were among the first to investigate the influence of strand geometry on panel strength. Post (1958) discovered that panels with longer strands tended to have high MOR value and found that the length to thickness ratio is directly correlated to strength. There are two modes of failure for wood strand panels shear at glue lines between strands and tensile capacity of individual strands (Suchsland, 1968).

As the length of the glue line increases the tensile capacity of the strands becomes the predominate model of failure. Shear lag analysis has been used to describe the stress transfer between discontinuous fiber composites by comparing the fiber maximum tensile strength and the maximum shear stress along the length of the fiber to determine the critical length of the fiber (Agaral & Broutman, 1980). Critical length of wood strands in OSB panels has been approximated to be 1mm (Yadama, 2006). A model by Barnes (2001) shows how stress transfer angles between contiguous strands in a wood strand composite is dependent on the length to thickness ratio (slenderness ratio) of the strands. Through the decrease in stress transfer angles between strands the shear strength of the glue line can increase.

Many strand and mat characteristics influence the mechanical properties of a wood strand panel. Barnes (2002) indicates a number of ways in which wood fiber orientation can deviate within a panel: deviation in grain angle within an individual strand, strand angle within a panel, and transfer of stress at an angle to the glue line. With a larger strand length longitudinal strength is increased and a better orientation of strands within a composite is achieved leading to even larger increases in longitudinal strength (Nelson, 1997).

Investigation of the influence of strand and mat parameters shows that improving strand geometry, strand orientation, and density can increase MOR and MOE (Wang & Lam, 1999). Density however has been shown to have the largest influence on mechanical properties (Wang & Lam, 1999, Meyers, 2001). Density can influence mechanical properties of strand composites in two ways: density variation in a population of panels, and density variation within individual panel (Bozo, 2002). Bozo (2002) showed that the density of commercially produced oriented strand board (OSB) panels had an average coefficient of variance (COV) of 6.67%.

Grain angle can have a significant impact on the strength properties of strand strength properties. Yadama (2002), Langum (2006), and the Wood Handbook (1999) all show a correlation between grain angle of wood and strength. Research by Yadama (2002) showed decreases in tension modulus of individual strands of nearly 60% when grain angle varied from 0 to 17 degrees. Barnes (2002) modeled the effect of grain angle and strand angle on tensile properties of oriented veneer and strand composites showing that

strand thickness and cross orientation of strands can influence the rate at which composite strength declines with increased alignment in grain and strand orientation angle.

PROJECT OBJECTIVES

The ability of any given strand mat to withstand a pultrusion process is greatly dependent on the strand mats tensile capacity. The tensile capacity of a strand composite depends on many variables including tensile properties of individual strand, strand geometry, and angle of grain in a strand. A proper characterization of strand and mat properties is important to improve the possibility of success of a strand pultrusion process. The specific objectives of this project are as follows:

- Quantify physical attributes of long (30 cm) strands from small diameter timbers using an industrial ring flaker.
- Perform tension tests on individual strands to determine mechanical properties.
- Produce and determine tensile properties of unidirectional composite panels at a range of densities using flat pressing techniques.

METHODS & MATERIALS

Strand Processing

Three commonly found species with large amounts of small diameter timbers in the Inland Pacific Northwest were used in this research. Grand fir (*Abies. grandis*), ponderosa pine (*Pinus ponderosa*), and lodgepole pine (*Pinus contorta*) timbers were chosen because of their availability and relative low-value. The timbers were harvested outside of Moscow, ID and had a breast height diameter ranging from 20 cm to 30cm.

The trees were cut into 2.5 m logs, debarked and stranded within 5 days of harvesting. Timbers were soaked in a conditioning pond for 12 hours prior to stranding. Strands were dried and then sorted using industrial disk attrition commonly found in oriented strand board manufacturing. From this process recovery data was generated.

Strand Physical Attribute Measuring

The dimensions of 120 strands of each species were measured using a digital caliper. Strands produced with the ring flaker showed large variations in dimensions and a large portion did not maintain a rectangular shape. To determine average strand dimensions all strands measured were assumed to be rectangular in shape.

The grain angle was also measured for each species utilizing a scribe to trace the grain angle in the strand. A high resolution digital image was taken of each specimen and then analyzed to measure the angle between the mark left by the scribe and the edge of the strand. Similar techniques have been used in past research (Yadama 2002, Langum 2006). A sample size of 80 strands per species was measured. Grain angle was measured with respect to the strand's x-axis (parallel to strand orientation).

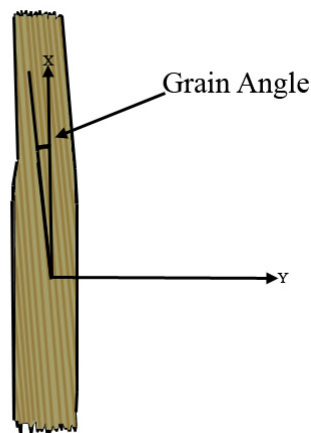


Figure 2.1- Grain angle measurement

Strand Tensile Testing

Strands were tested in tension to determine tensile modulus and ultimate tensile strength of each species. Rectangular tension specimens with dimensions of 25.4 mm by 254 mm were cut from the strands. 80 tension specimens of each of the three species were conditioned at 22 degrees C and 50% relative humidity for one week. A 9-kN screw driven universal testing machine was used to test each specimen. Within the testing machine vertically aligned grips attach to either side of a specimen. The testing machine then applied a load to the specimens and recorded the applied load. The load was applied at a rate of 1.02 mm per minute. A 1.25 cm extensometer was used to measure strain in the specimens during testing. The recorded load and deformation were then used to determine the tension modulus and ultimate tensile strength. All tension specimens with failures at or near the aligned grips were deemed unusable for the calculation of mechanical properties.

Specific gravity of each tensile specimen was calculated based on ASTM Standard 2395 method A, which uses the measured dimensions and weight of the rectangular tensile specimens. A moisture content of 12% was used in determining the specific gravity.

Unidirectional Strand Composite Manufacture

A press schedule was developed to emulate the closing and dwell time expected during a continuous pultrusion. The press schedule is as follows: first the press platens closed

rapidly to a 76.2 mm opening, over the next 280 seconds the press platens were closed to a final thickness of 9.5 mm, the press was then held at 9.5 mm for 360 seconds, released to 10.7 mm in 40 seconds and to 12.7 mm in 40 seconds. Platen temperatures were held constant at 142 degrees C throughout the entire process. Panels were produced with each of the three species and at densities of 560.6, 680.8, and 800.9 g/m³. Panel dimensions of 101.6 mm x 863.6 mm were chosen to emulate the pultruded composite dimensions and the mass and heat transfer likely to occur in the wood strand pultrusion process.

To form mats with such long and narrow dimensions and reduce the amount of waste generated in the form of panel edges a unique mat forming process was developed. In this process strands were first dried to a moisture content below 5%. Strands were then sprayed with a liquid PF surface resin for OSB (Product code: 2161-4-LPF-Face) provided by ArclinTM at a 6 % resin solids loading. Mats were formed uni-directionally using an oscillating forming box with a vane spacing of 76 mm resulting in a 495 mm x 864 mm panel. The mats were then pre-pressed between two sheets of oriented strand board (OSB) and screwed together. The strand mat and OSB together were then cut into three 102 mm strips on a table saw. 95 mm of edge material was cut off and discarded. The OSB was removed leaving a 102 mm by 864 mm mat strip. Each mat strip was then individually pressed at the above mentioned press parameters.

Unidirectional Strand Composite Testing

Prototype strand composites were tested in tension to determine tensile modulus and ultimate tensile strength of each species and density. The panels were cut into dog bone tension specimens with dimensions of 610 mm by 76 mm. Fifteen specimens for each

combination of species and density were then conditioned at a temperature of 21 degrees C and 50% relative humidity for one week.

A 133-kN screw driven universal testing machine was used for tension test of strand composites based on ASTM Standard 1037. The load was applied at a rate of 3.8 mm per minute as specified in ASTM Standard 1037. A 102 mm LVDT was used to measure strain within the 152 mm gauge length of the specimen. Load recorded from the testing machine and strain recorded from the extensometer was used to calculate tension modulus and ultimate strength.

Statistical Analysis

Cumulative frequency plots can be utilized to display graphically the distribution of parameters. General linear models (GLM) and Duncan tests are statistical procedures for determining if a parameter X has a significant influence on a parameter Y in a data set. The GLM used is a statistical model that uses matrices to compare parameters in a data set by incorporating analysis of covariance (ANCOVA) statistical models, linear regression techniques, t-tests and F-tests. ANCOVA will determine if the covariate is significant, but it also states whether a covariate is significant without the influence of the other covariate. Eliminating the influence of covariates is done through linear interpolation (Lyman Ott, 1993). A Duncan test utilizes studentized range statistics to compare sets of mean values in a multiple comparison procedure (Lyman Ott, 1993).

RESULTS & DISCUSSION

Strand Geometry

The results from the measurement of the strand dimensions can be seen in Table 2.1. The ratio of the strand length to the strand thickness (slenderness ratio) was also calculated and is shown in Table 2.1.

Table 2-1- Average strand dimensions

	Ponderosa Pine	Lodgepole Pine	Grand Fir
Length (mm)	283 ^A (41)	267 ^B (53)	253 ^C (58)
Width (mm)	27 ^A (14)	26 ^A (17)	14 ^B (10)
Thickness (mm)	0.81 ^A (0.70)	0.75 ^A (0.20)	0.78 ^A (0.18)
Slenderness Ratio	392 ^A (99)	377 ^A (111)	343 ^B (109)

*Values in parenthesis denote standard deviation

*Superscripts denote Duncan classification

General linear modeling procedures and Duncan tests were utilized to determine the significance of species on strand dimensions. Strand length showed a significant difference between all three species. Strand width and slenderness ratio showed no significant difference between lodgepole pine and ponderosa pine, but a significant difference was observed between grand fir and the two pine species. No significant difference was observed between the thicknesses of the three species. The results of the GLM procedure and Duncan tests for strand dimensions can be found in the Appendix A. Figure 2.2 and 2.3 show the cumulative frequency plot for the slenderness ratio and strand width for each species. Cumulative frequency plots for all strand dimensions are shown in Appendix B.

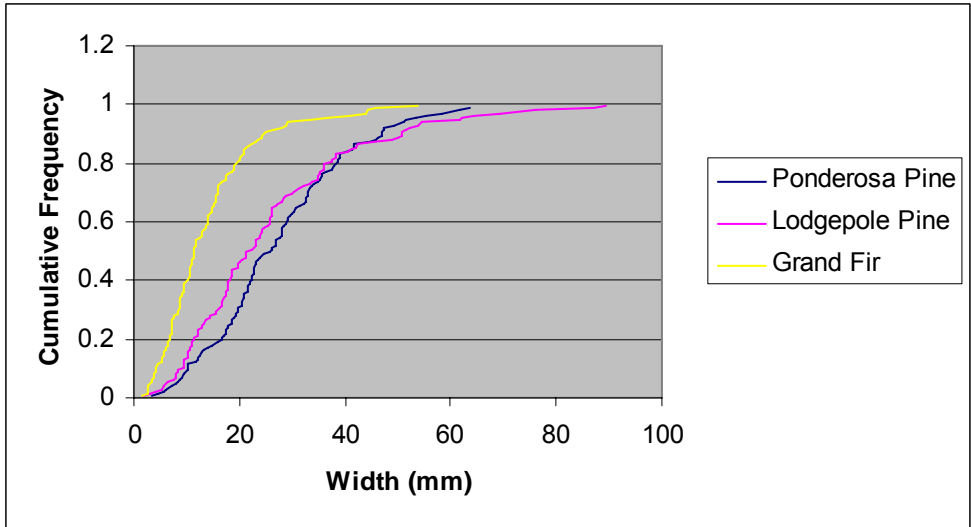


Figure 2.2 - Cumulative plot for strand width

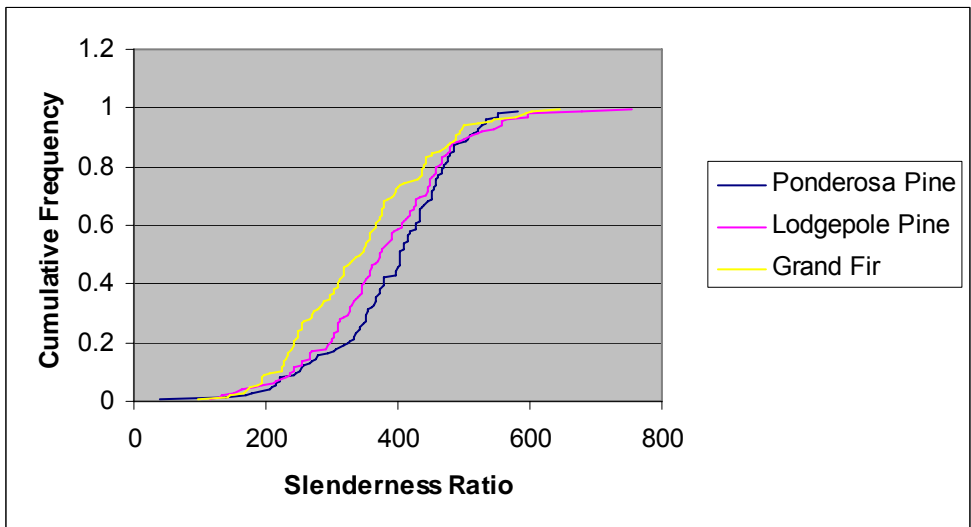


Figure 2.3 - Cumulative plot for slenderness ratio

Grain Angle

Grain angle measurements were taken from 80 specimens per species. The grain angle measurements represent the angle (in degrees) measured between the grain of the strand and the x-axis of the strand (parallel to the edge of the strand). Figure 2.4 shows cumulative plots for grain angle of each species.

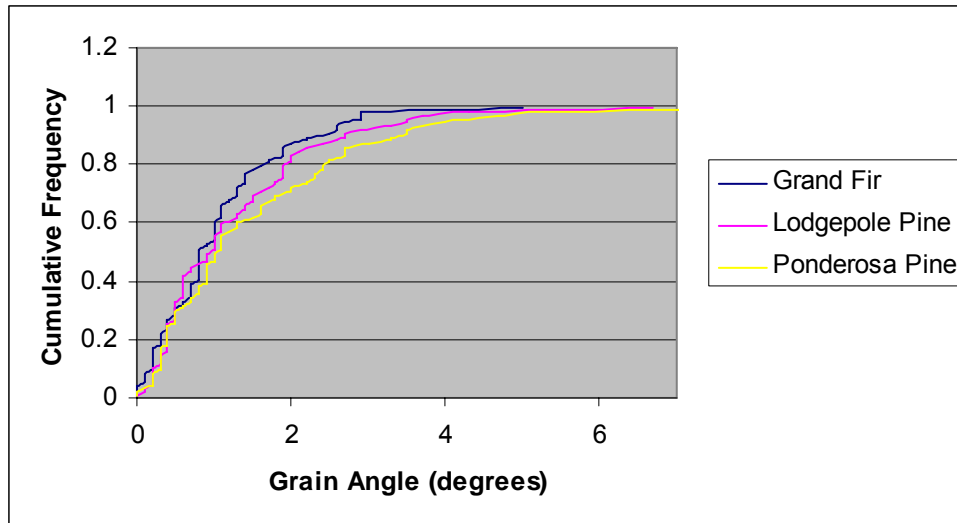


Figure 2.4 -Cumulative plot of grain angle

The distribution of grain angles in this study shows that strands of each species were very well aligned and little variation between species. A GLM procedure and Duncan test were ran to determine the significance of species on grain angle. A significant difference in grain angle was observed between grand fir and ponderosa pine, but there was not a significant difference between grand fir and lodgepole pine or between lodgepole pine and ponderosa pine. The results of the GLM procedure and Duncan tests for grain angle can be found in the Appendix C.

Compared to grain angles in strands in other studies (Yadama, 2002 and Langum, 2006) the grain angle in strands found in this study showed very straight alignment. Factors that could have contributed to the alignment of the grain angle are the type of strander used, fewer knots in the original timbers, and the straightness of the original timbers. The low sample size of small diameter timbers used in this research provides low confidence that the grain angle in strands in this research is representative of the global population of

small diameter timbers. Even though the grain angle in strands do not provide a high confidence there is consistency between species in the study.

Strand tensile properties

The tension modulus and ultimate tensile strength of individual strands was tested for each of the three species (Table 2.2).

Table 2-2- Strand tensile properties

	Ponderosa Pine	Lodgepole Pine	Grand Fir
Ultimate Tensile Strength (MPa)	40.62 ^A (14.51)	35.86 ^B (14.28)	43.50 ^A (15.20)
Tension Modulus (GPa)	8.051 ^B (1.630)	7.740 ^C (2.490)	8.556 ^A (1.774)
Specific Gravity	0.32 (0.04)	0.33 (0.04)	0.29 (0.03)

*Values in parenthesis denote standard deviation

*Superscripts denote Duncan classification

Figure 2.5 and 2.6 show the cumulative plots for ultimate tensile strength and tension modulus for each species.

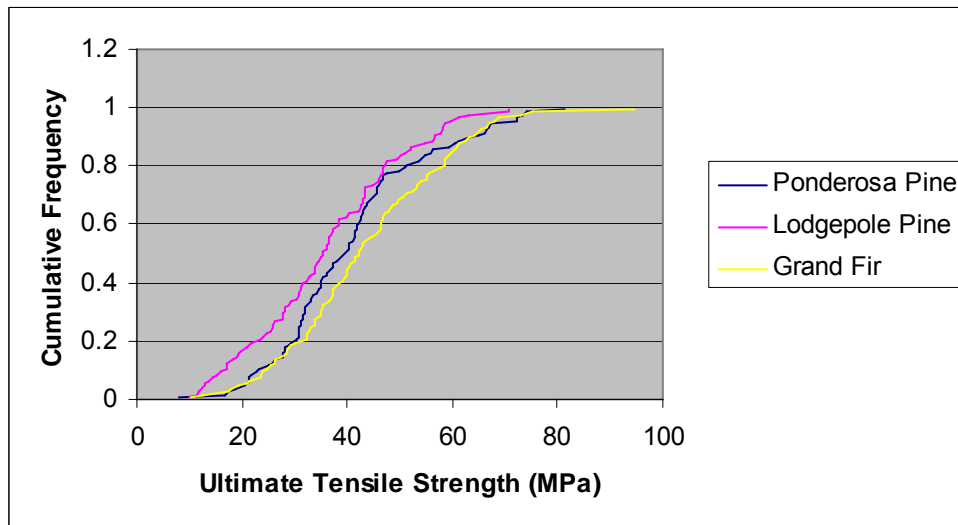


Figure 2.5- Cumulative plot of ultimate tensile strength

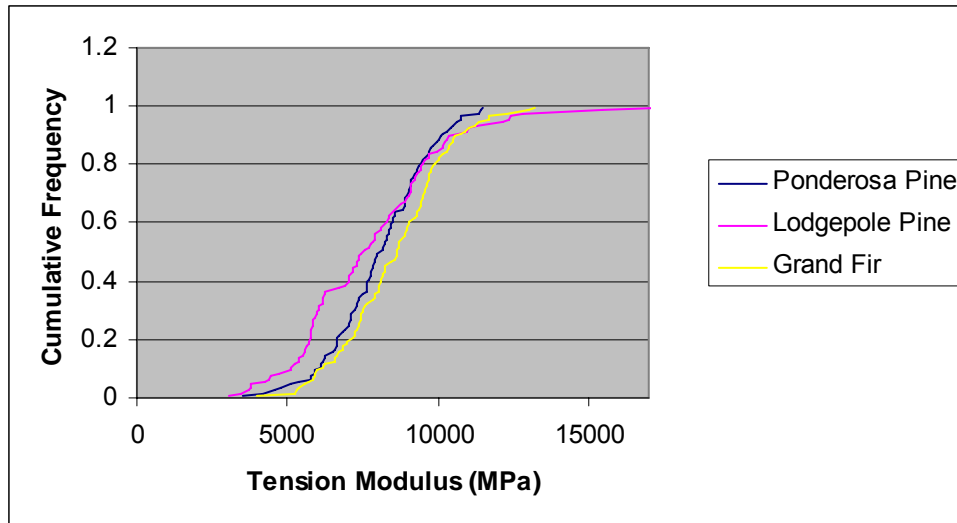


Figure 2.6- Cumulative plot of tension modulus

An analysis of covariance (ANCOVA) procedure with a Duncan means test was run to determine the significance of species on ultimate tensile strength, and tension modulus, with specific gravity as a covariate. The ANCOVA procedure showed that species and specific gravity have a significant influence on ultimate tensile strength and tension modulus. The Duncan test showed a significant difference between species, except in the case of tension modulus where little significance was noticed between grand fir and ponderosa pine. The average tension modulus and average ultimate tensile strength for grand fir were both slightly larger than ponderosa pine, and lodgepole pine. Results of the GLM procedure, Duncan tests for the tensile properties of strands can be found in Appendix D.

Ultimate tensile strength average values were compared to average values of MOR from the ASTM Standard D2555 as allowed by section 2.4 of the standard. Figure 2.7 shows comparisons of ultimate tensile strength found in this research to average values of MOR from ASTM Standard D2555.

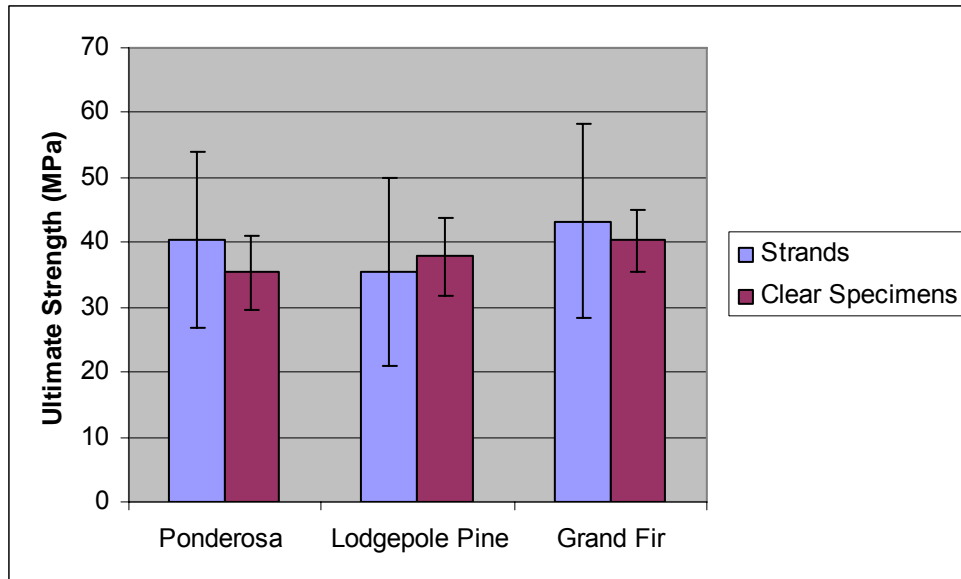


Figure 2.7- Comparison of ultimate tensile strength values with values form ASTM Standard D2555

Ponderosa pine and grand fir show the ultimate tensile strength exceeds the tensile capacity of clear span MOR values. All three species are with the standard deviation of the values form ASTM Standard D2555.

Processing data

The ability to successfully convert timber into strands at a high recovery rate is very important. If only a small percentage of each timber that is stranded can be converted into usable material then the process is not a cost effective use of the timbers. The percentage of usable strands is defined as the amount of usable strands divided by the total number of strands produced. Figure 2.8 shows the percentage of usable strands recovered from the stranding process which uses an industrial disk attrition system commonly found in oriented strand board manufacturing.

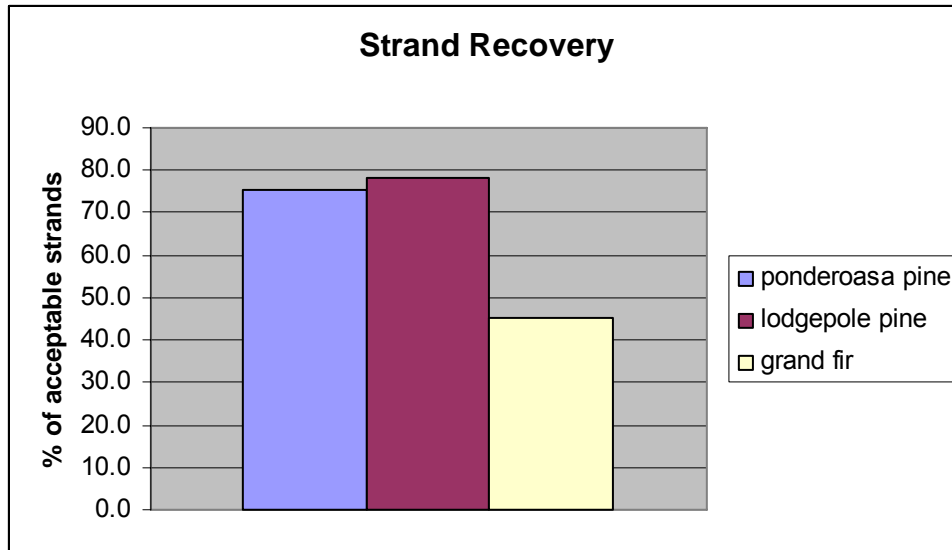


Figure 2.8 - Percentage of accepted strands from stranding process

Figure 2.8 shows that there was a significantly lower amount of usable grand fir strands than that of ponderosa pine and lodgepole pine. Average strand length and width could influence the acceptance of strand due to the disk attrition sorting process.

Composite tensile properties

Prototype panels were tested in tension to determine the ultimate tensile strength and tension modulus. Table 2.3 shows average ultimate tensile strength and tension modulus for each species and target density. The small sample size for each species and target density does not allow for an accurate use of statistical distributions; however ANCOVA procedures with density as a covariate were used to determine significance with species. Density significantly influenced both tension modulus and ultimate tensile strength while species significantly influenced ultimate tensile strength but not tension modulus. Target density significantly influenced tension modulus but not ultimate tensile strength.

Table 2-3 - Average tensile properties of composites

Species	Target Density (kg/m ³)	Density (kg/m ³)	Average Tension Modulus (GPa)	Average Ultimate Tensile Strength (MPa)
Ponderosa Pine	560	622 (71)	7.660 (3.730)	36.10 (18.43)
	680	631 (42)	12.045 (4.854)	24.88 (7.53)
	801	818 (39)	15.844 (7.639)	58.99 (10.34)
Lodgepole Pine	560	567 (45)	10.439 (4.116)	28.84 (10.18)
	680	692 (42)	15.624 (7.467)	39.67 (13.38)
	801	748 (23)	9.184 (1.186)	40.87 (15.42)
Grand Fir	560	614 (47)	7.074 (2.765)	25.06 (8.22)
	680	642 (49)	12.466 (4.323)	31.00 (7.07)
	801	883 (47)	14.224 (6.778)	43.13 (9.32)

*Values in parenthesis denote standard deviation

Figure 2.9 and 2.10 show the relationship between tension modulus and density and ultimate tensile strength and density. Linear regression (Least squares method) curves were fit to the ultimate tensile strength and density relationship and the tension modulus and density relationship.

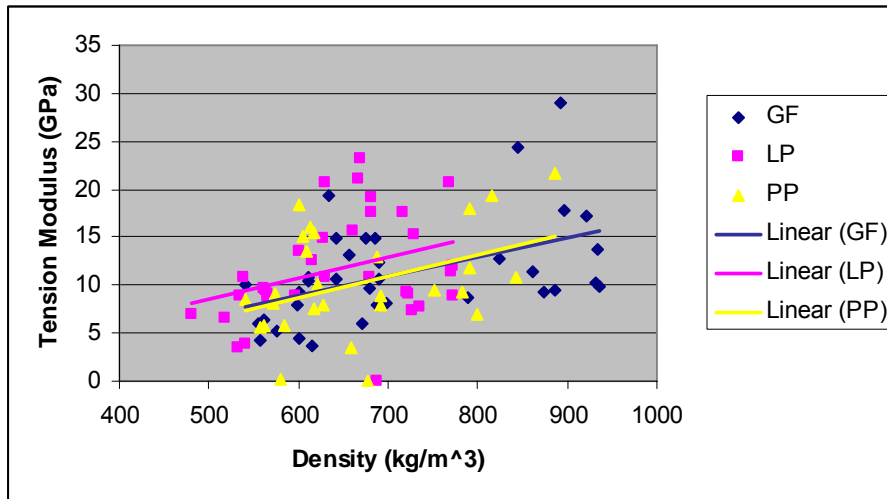


Figure 2.9 -Composite ultimate tension modulus with density

Past research (Meyers, 2001, Bozo, 2002) shows density has a pronounced effect on ultimate tensile capacity. The change in ultimate tensile strength with density was quite similar in both grand fir and lodgepole pine. Even though grand fir showed slightly larger ultimate tensile strength in individual strands, the smaller strand width coupled

with the 76 mm vane width could have resulted in a larger variation in in-plane strand angle within the mat and contributed to lower composite properties. The R^2 terms for the trend lines in Figures 2.9 and 2.10 are can be found in the Appendix E.

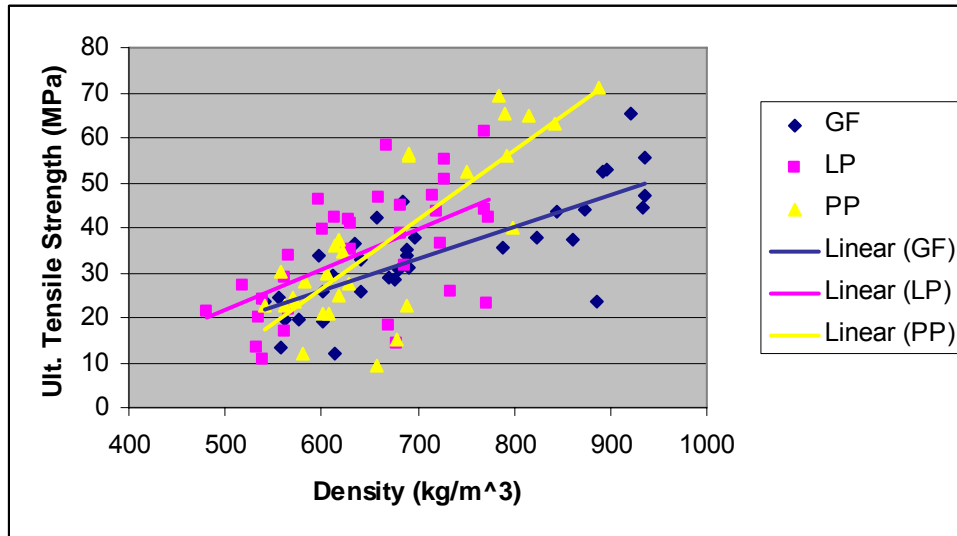


Figure 2.10- Composite ultimate tensile strength with density

The change in tension modulus with density was quite similar in each species. Grand fir and ponderosa pine both showed smaller tension modulus then lodgepole pine.

CONCLUSIONS

Strands were generated from three under-utilized species of small diameter timbers (ponderosa pine, lodgepole pine, and grand fir) using an industrial ring flaker. The strands that were produced from the three species all had lengths in the desired range of 20 mm to 30 mm. Strand physical properties were measured, calculated and analyzed to determine there influence on tensile properties and dependence on species. All three species had dimensions ranging from 280mm to 250mm in length, 27mm to 14mm in width, and an average thickness of 0.8mm. Strand dimensions all showed some significant differences between species, except of strand thickness. Species in this

research had an average strand grain angle of 1.25 degrees. Strand grain angle was well aligned when compared to previous research (Yadama 2002, Langum 2006). Species was shown to have a slight influence on the strand grain angle.

Mechanical properties of individual strands and composites were tested, calculated, and analyzed to determine the influence of density, and species. Tensile testing of individual strands showed average ultimate tensile strengths ranging from 44 MPa to 36 MPa and tension moduli ranging from 7.7 GPa to 8.6 GPa. Species and specific gravity were found to have a significant influence on strand tensile properties. An ANCOVA procedure was used to determine that the two covariants influence was independent of one another. Strand ultimate tensile strength compared well to values of MOR for ASTM Standard D2555.

Prototype uni-directional panels were produced at the desired range of densities using flat pressing techniques and were tested for tensile properties. Tensile properties were analyzed to determine the influence of species type and density. The tensile properties of the strand composites showed an influence of density and species, especially with respect to density. Processing recovery data showed that grand fir yields a much smaller amount of usable strands than lodgepole and ponderosa pine.

REFERENCES

Agarwal, Bhagwan D., and Lawrence J. Broutman. *Analysis and Performance of Fiber Composites*. New York: John Wiley & Sons, Inc., 1980.

ASTM Standard D1037 A Standard Test Method for Evaluating Properties of Wood-Base Fiber and Particle Panel Materials. American Society for Testing and Materials, 2007.

ASTM Standard D2395 Standard Test Methods for Specific Gravity of Wood and Wood-Based Materials. American Society for Testing and Materials, 2007.

ASTM Standard D2555 Standard Test Methods for Establishing Clear Wood Strength Values. American Society for Testing and Materials, 2007.

Barnes, Derek. "A model of the effect of strand angle and grain angle on the strength properties of oriented veneer and strand wood composites." *Forest Products Journal* 52.4 (2002): 39-47.

---. "A model of the effect of strand length and strand thickness on the strength properties of oriented wood composites." *Forest Products Journal* 51.2 (2001): 36-46.

Bozo, Alejandro M. "Spatial Variation of Wood Composites." Aug 2002. Thesis. Washington State University

Langum, Christopher E. "Characterization of Pacific Northwest softwoods for wood composite production." May 2007. Thesis. Washington State University

Lyman Ott, R. *An Introduction to statistical methods and data analysis.* Belmont, CA: Duxbury Press, 1993.

Meyers, Kristin Lynne. "Impact of strand geometry and orientation on mechanical properties of strand composites." Dec 2001: 22-43. Thesis. Washington State University

Nelson, Sherman. "Chapter 6: Structural Composite Lumber." *Engineered Wood Products: A guide for specifiers, designers and users*. Ed. Stephen Smulski. Madison, WI: PFS Research Foundation, 1997. 6-147 to 6-172.

Post, P.W. "Effect of particle geometry and resin content on bending strength of oak flake board." *Forest Products Journal* (1958): 317-322.

Suchsland, Otto. "Particle-board from southern pine." *Southern Lumberman* (1968): 139-144.

Wang, Kaiyuan, and Frank Lam. "Quadratic RSM models of processing parameters for three-layer oriented flakeboard." *Wood and Fiber Science* 31.2 (1999): 173-186.

Wood Handbook, Wood as an Engineered Material. Forest Products Laboratory, 1999.

Yadama, Vikram. "CE 437 Wood Composites." October 17, 2006. Lecture. Washington State University

---. "Characterization and modeling of oriented strand composites." Dec 2002: 102-133. Thesis. Washington State University

CHAPTER 3 : FEASIBILITY OF PRODUCING PULTRUDED LONG STRAND COMPOSITES

ABSTRACT

The use of pultrusion processes to produce long strand composite could allow for the development of new light weight structural composites with variable profiles. During the pultrusion of a long strand composite large pulling forces are developed as the mat is compressed and formed into a final profile. Proper modeling of these pulling forces is crucial in the success of a wood strand pultrusion operation. A model was developed that describes the consolidation and ensuing relaxation of stress for strand mats based upon the processing parameters of the pultrusion die to determine the accumulated pulling force. Consolidation data was gathered by creating prototype panels using flat pressing techniques and was modeled utilizing existing models that predict the compressive response of strand mats. A pultrusion process for wood strand composites was developed to verify the pulling force model.

INTRODUCTION

The feasibility of a strand composite pultrusion process is based on one basic inequality; tensile capacity of the composite must be greater than the pulling force developed in the pultrusion die. An estimate of the tensile capacity of the composite can be determined through the production and testing of prototype composites produced with flat pressing techniques. To determine an accurate prediction of the pulling force a model can be

developed that accounts for all forces that are applied to the composite during processing. A pulling force model is also an important tool for evaluating the influence of processing parameters and material characteristics on the pulling force. Processing parameters that could influence the pultrusion process include the die geometry, pulling rate, die temperature, and the frictional coefficient of the steel die and the wood strand mat.

In order to better understand the development of the pulling force model the pultrusion process must first be understood. The pultrusion process used in this research is similar to standard pultrusion processes used throughout industry with a few modifications.

Figure 3.1 below shows the entire process. First a strand mat is conveyed into the heated pultrusion die by means of a belt conveyor. The die has two sections: a tapered entrance section where the composite is consolidated to the desired profile, and a constant geometry section where the composite is held in its final profile while the thermoset resin is able to cure. After exiting the die the composite reaches the puller. The puller is the driving force of the process pulling the composite through the die. Finally the composite is cut into pre-determined lengths with a cut off saw.

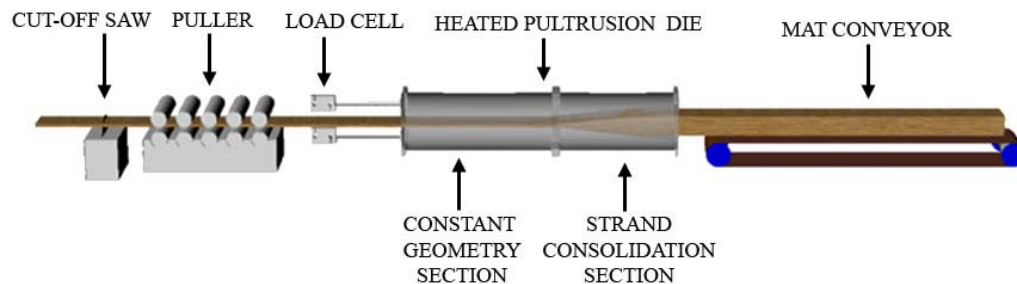


Figure 3.1 - Pultrusion process overview

The forces contributing to the pulling load are the frictional and normal forces developed from the strand consolidation and relaxation stresses associated with mat compression. The above mentioned forces can further be divided into three sets: normal forces due to consolidation stresses in the entrances section, frictional forces due to consolidation stresses in the entrance section, and frictional forces due to relaxation stresses in the constant geometry section (Figure 3.2).

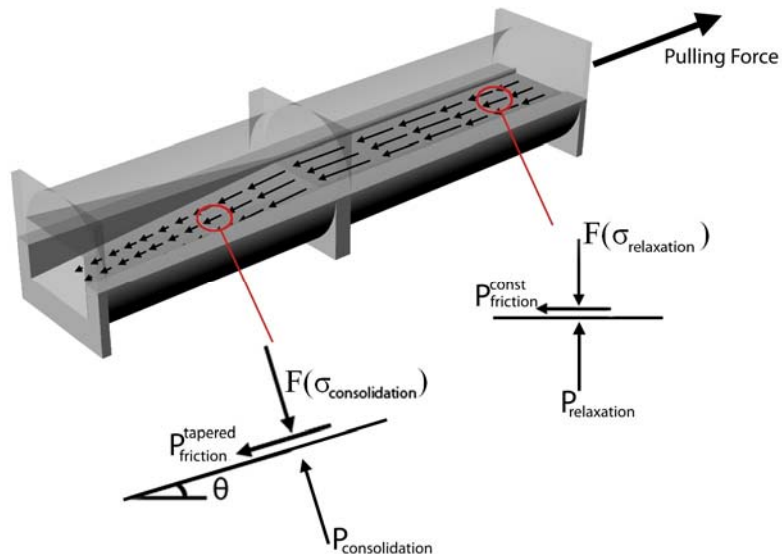


Figure 3.2 -Friction & normal forces in the pultrusion die

A similar model was developed by Englund (2001) to predict the pulling force developed in a fibrous mat pultrusion process. The basic concept of this model can be used to model the pulling force of pultruded strand mats.

Compression of panel products

Wood composites are drastically different than synthetic composites in a number of ways. Wood composites contain small amounts of thermoset resins and require large compressive forces to densify their mat structure when developing their strength

properties. This compaction process results in the permanent deformation of the wood particles. Synthetic composites typically contain large amounts of thermoset resin forming a resin matrix. The use of large amounts of resin requires little compressive force and little to no densification of the composite (Dai & Steiner, 1993). In reference to pultrusion the difference between wood and non wood composites requires a solid mechanics approach rather than a fluid mechanics approach to describe the material behavior during processing (Englund, 2001).

To understand the consolidation of a strand composite in a pultrusion process a basic knowledge of the compaction pressure applied to the strand mat during flat pressing is needed. The typical compaction curve has four regions: press closure, transient relaxation, asymptotic relaxation, and venting (Wolcott, 1990). Figure 3.3 shows these four regions. The press closure can be predicted using a variety of models that relate mat density and compaction or consolidation pressure. Transient and asymptotic relaxation can be modeled together using Maxwell elements that relate the relaxation stress to press time. The modeling of both press closure and relaxation will be discussed in detail later in this chapter.

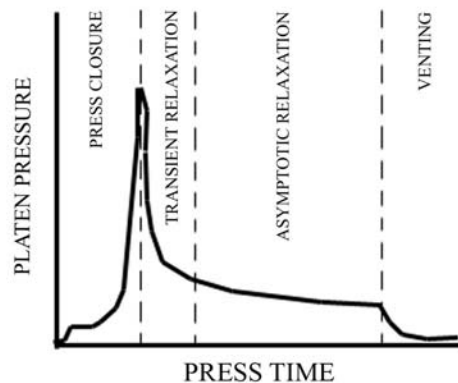


Figure 3.3- Compaction pressure during flat pressing (Wolcott, 1990)

Consolidation Stress

There are a number of models that have been developed to predict the consolidation behavior of wood strand mats. Dai & Steiner (1993) developed a theoretical based model for the consolidation of flake board mats. A modified Hooke's law with a non-linear strain function was used to describe the consolidation stresses of wood strands in mat structures. By describing the mat structure as infinitely small rectangular columns and using a Poisson's distribution function to predict the number of strand in each column the model was able to predict the consolidation stresses in the higher stress regions with good accuracy. Wolcott & Lang (1996) developed a similar model for prediction of mat consolidation behavior. By incorporating a Monte Carlo simulation the consolidation stresses from strand bending that dominate the low stress regions of mat consolidation were modeled with good accuracy. A model by Length & Kamke (1996) incorporated theories of cellular materials, and accurately predicted the consolidation stresses developed in the lower stress regions, but had some trouble predicting stresses in the higher stress regions.

Recently Zhou & Dai (2008) have developed a new generalized model for the prediction of consolidation in all wood composites. This model predicts the consolidation of wood composites by analyzing the bending of wood fibers in different types of mats. Accurate predictions of the consolidation of different types of wood composites were made using this model. When coupled with Dai & Steiner's (1993) model for the compressive

behavior of wood flake mats provides a simple and accurate description of the consolidation stresses developed in a strand mat.

Even with the abundant amount of research dedicated to modeling the behavior of strand mats there is still some difference between past models and a model needed for the wood strand-based pultrusion process. Many past models only predict the consolidation at ambient temperatures, which does not take into account heat and mass transfer. Past models also predict the consolidation of randomly oriented strand mats, and not the consolidation of uni-directional strand mats.

Relaxation Stress

The relaxation behavior associated with the hot pressing of wood strand mats is a very complex process; also the relaxation behavior has little use in the wood composites industry. It is for these reasons that little theoretical modeling has been done to predict this relaxation behavior of strand mats. A simple spring and dashpot model can be used to represent the viscoelastic behavior of strand mats under compressive loads. A set of spring and dashpots in series, commonly known as Maxwell elements, have been used in the past for such modeling (Malvern, 1969). A similar model was used to model the relaxation stress in wood fibrous mats in a pultrusion process by Englund (2001).

Friction

Friction is a parameter that is rarely needed in the production of wood composites, but is crucial in a wood or solids based pultrusion process. The dynamic coefficient of friction has been shown to be dependent on many factors including temperature, and normal force (Englund, 2001). Research by Englund (2001) tested the static and dynamic coefficients

of friction of fibrous mats and solid wood. The test procedure used a load cell to apply a normal force to a set of heated platens. Between the heated platens were two test specimens with a pulling block attached in between the two test specimens. The pulling block and specimens were then pulled out from between the heated platens. The force required to move the pulling block and the normal force applied to the heated platens were then used to calculate the coefficients of frictions at a range of dwell times, temperatures, and normal force.

OBJECTIVES

An accurate prediction of pulling force developed in the pultrusion die is essential in determining the feasibility of pultruding a wood composite. The specific objectives of this project are as follows:

- Experimentally measure the compressive stresses developed during mat consolidation of uni-directional long strand mats of varying species and density.
- Predict the mat consolidation and relaxation response of uni-directional strand mats using existing models.
- Determine the coefficient of friction for strand composites by utilizing wood veneer and determine the influence of platen temperature and applied normal load.
- Develop a model for predicting the pulling force caused by normal and frictional forces developed in the pultrusion die.
- Design and construct a pultrusion process for wood strand mats.

MODEL DEVELOPMENT

The pulling force model incorporates the geometry of the pultrusion die and the consolidation and relaxation stresses in the composite to determine a prediction of the pulling force. The pulling force model in this research is based on the pulling force model developed by Englund (2001) for wood fibrous mats.

Modeling of Pulling Force

The modeling of the total pulling force can be subdivided into two types of forces: frictional and normal forces. The two types of forces can result from two types for compressive stresses of the strand mat: consolidation stresses and relaxation stresses. The consolidation stresses are developed in the entrance section of the pultrusion die where the strand composite is compressed to the final profile. The relaxation stresses are developed in the constant geometry section of the pultrusion die where the thermoset resin is permitted to fully cure.

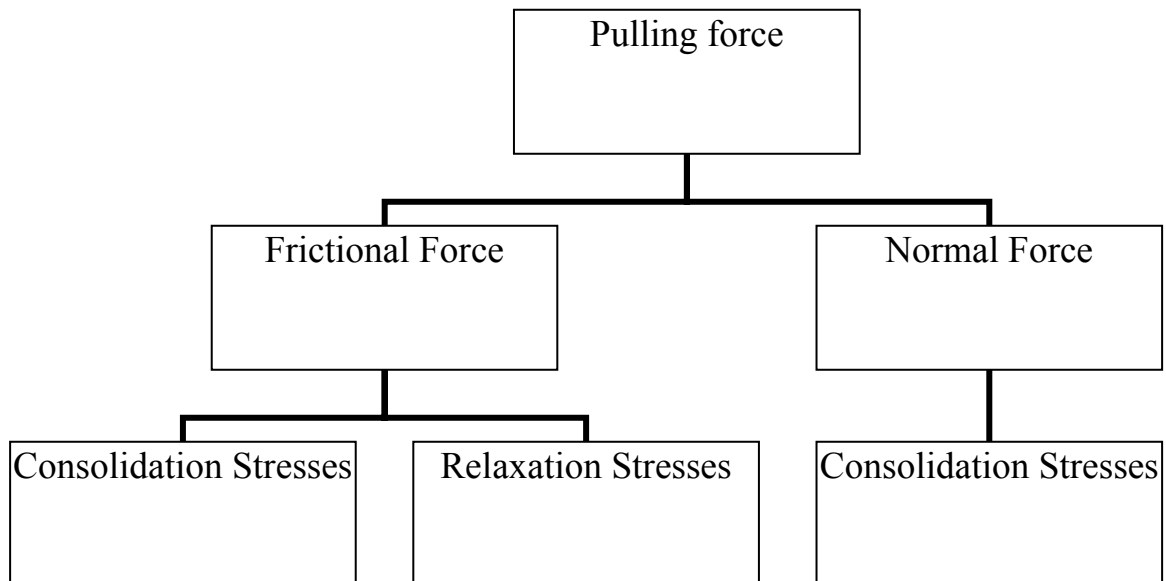


Figure 3.4 - Overview development in pultrusion die

Therefore the resulting pulling force is the sum of the normal force due to consolidation stress in the entrance section , frictional force due to the consolidation stress in the entrance section, and frictional force due to the relaxation stress in the constant geometry section. The frictional force due to consolidation stresses and relaxation stresses are only calculated for the frictional force on one surface of the strand composite and therefore is doubled in the summation of the total pulling force (Eq 3.1).

$$P_{tot} = 2[(Px_{con})_{frict} + (Px_{ent})_{frict}] + Px_{con} \quad \text{Eq.3.1}$$

Where: P_{tot} = total pulling force

$(Px_{con})_{frict}$ = friction force in the constant geometry section

$(Px_{ent})_{frict}$ = friction force in the entrance section

Px_{con} = normal force due to consolidation

Accumulation of pulling force along the length of the die determined by integrating along its length will equal the total pulling force. Accumulated pulling force will be useful in determining the feasibility of a wood strand pultrusion process.

Normal force due to consolidation stresses in the entrance section Px_{con} is calculated by integrating the horizontal component of the consolidation stress (σ_c) multiplied by the width of the strand composite over the length of the entrance section.

$$Px_{con} = \int_0^{L_c} w \sigma_c \sin \theta dx \quad \text{Eq.3.2}$$

Where: L_c = length of the entrance section

w = width of pultrusion profile

σ_c = consolidation stress

θ = the angle of the entrance section

Frictional force due to consolidation stresses in the entrance section $(P_{x_{ent}})_{frict}$ is calculated by integrating the vertical component of the consolidation stress (σ_c) multiplied by the width of the strand composite and the dynamic frictional coefficient μ_k over the length of the entrance section.

$$(P_{x_{ent}})_{frict} = \int_0^{L_c} w \sigma_c \mu_k \cos \theta dx \quad \text{Eq.3.3}$$

Where: L_c = length of the entrance section

w = width of pultrusion profile

σ_c = consolidation stress

μ_k = coefficient of friction

θ = the angle of the entrance section

The consolidation stress (σ_c) is modeled from the compression data collected during the flat pressing of prototype panels. The modeling of the consolidation stress will be discussed in detail in the modeling of consolidation stress section.

Frictional force due to relaxation stresses in the constant geometry section $(P_{x_{con}})_{frict}$ is calculated by integrating the relaxation stress (σ_r) multiplied by the dynamic coefficient of friction μ_k and the width of the composite over the length of the constant geometry section. A diagram of all three forces is shown in Figure 3.2.

$$(P_{x_{con}})_{frict} = \int_0^L w \sigma_r \mu_k dx \quad \text{Eq.3.4}$$

Where: L = length of the constant geometry section

w = width of pultrusion profile

σ_r = relaxation stress

μ_k = coefficient of friction

The relaxation stress will be determined using compression data collected during the flat pressing of prototype panels and a relaxation stress model. The relaxation stress will be discussed in detail in the modeling of relaxation stress section.

There are many assumptions made in developing the pulling force model.

- The dynamic coefficient of friction is constant throughout the heated die. There is a possibility that the dynamic coefficient of friction between the composite and the die could change as the thermoset resin is cured.
- The dynamic coefficient of friction of wood veneers is equal to the dynamic coefficient of friction of strand mats.
- Forces resulting from contact of the strand composite and the vertical surfaces of the die are minimal and can be neglected. In order to insure that there is no contact of the composite and the vertical surfaces of the die the width of the composite has been reduced.

Modeling of Consolidation Stresses

Consolidation of strand mats is a well researched area. A modified Hookean relationship with a non-linear strain function is a common way to predict the consolidation stress developed in strand mats (Dai & Steiner 1993, Wolcott et al 1994, Lenth & Kamke, 1996). For this research a generalized mat consolidation model for wood composites is

used (Zhou & Dai, 2008). This model was chosen based on its simple nature and its ability to be used for a wide range of wood composites other than strands.

When used to predict the consolidation forces in strand mats Zhou & Dai (2008) determined that the consolidation force is best modeled as two separate components bending of individual strands and transverse compression of wood strands. The bending component is accurate for low stresses and the compression component is accurate for higher stresses. Zhou & Dai (2008) determined that the point at which the consolidation changes from bending of individual strands to compression of wood strands is near the initial density of the strands.

The bending component models the strand mat as a random system of two-dimensional bending units. Using beam deflection relationships along with strand geometry the following semi-empirical equation was derived.

$$\sigma_c = \frac{KE_s}{\rho_s^n} (\rho_m^n - \rho_0^n) \quad \text{Eq.3.5}$$

Where: σ_c = compressive stress

K = experimentally determined factor

E_s = elastic modulus of individual strands

n = exponent based on mat type

ρ_s = individual strand average density

ρ_m = mat density

ρ_0 = initial mat density

In this equation K is an experimentally determined factor that corrects for orientation of strands within a mat, variation in strand dimension, and variation in bending length.

The compression component is a model developed by Dai and Steiner (1993). The consolidation is modeled as a system of infinitely small columns with varying amount of strands in each column. The probability of n strands existing in each column is described by a Poisson's distribution.

$$p(i) = \frac{a_i}{A} = \frac{e^{-n} n^i}{i!} \quad \text{Eq.3.6}$$

Where: $p(i)$ = probability of i flakes existing in a column

a_i = individual strand average area

A = mat area

n = mean number of flakes in a column

i = number of flakes in any given column

The total compressive stress is then calculated using a modified Hookean relationship as shown in Eq 3.7. In Eq 3.7 the compressive stress is related to mat density through the mean number of flakes in a column, n , which can be calculated using the individual strand average area, the number of strands in the mat, and the mat area.

$$\sigma_c = E_c e^{-n} \sum_{i=T/\tau}^{\infty} \phi(\varepsilon_i) \varepsilon_i \frac{n^i}{i!} \quad \text{Eq.3.7}$$

Where: σ_c = compressive stress

E = compression modulus

n = mean number of flakes in a column

i = number of flakes in any given column

$\varphi(\varepsilon_i)$ = straining function for a column with i flakes

ε_i = strain in a column with i flakes

Modeling of Relaxation Stresses

Relaxation stresses of the strand mat were modeled using a generalized Maxwell model.

A generalized Maxwell model is a set of parallel aligned Maxwell elements. Each Maxwell element consists of a spring and dash-pot aligned in series. Spring and dash-pot models are commonly used to describe a qualitative representation of the viscoelastic behavior (Malvern, 1969). The general differential equation for a Maxwell model is as follows:

$$\frac{d\sigma_r}{dt} = E \frac{d\varepsilon}{dt} + \frac{\sigma_r}{\lambda} \quad \text{Eq.3.8}$$

Where λ is the relaxation time (Christensen, 1971), and E is the elastic modulus. The solution to the differential equation is shown as Equation 3.9. Based on previous research (Englund, 2001) a four parameter Maxwell model was used in modeling the relaxation modulus.

$$E(t) = \sum_{i=1}^4 E_i e^{-t/\lambda_i} \quad \text{Eq.3.9}$$

$$\sigma_r = \varepsilon_0 \sum_{i=1}^4 E_i e^{-t/\lambda_i} \quad \text{Eq.3.10}$$

Where: E(t) = elastic modulus at time t

E_i = elastic modulus at time λ_i

λ_i = relaxation time

σ_r = relaxation stress

ε_0 = initial mat strain

When a constant strain ε_0 is applied to a strand mat the compressive stress σ_r decreases over time (Englund, 2001). The relaxation modulus $E(t)$ can then be defined as σ_r / ε_0 (Englund, 2001). Combining the two relationships for relaxation modulus and solving the equation for the relaxation stress, σ_r , yields an equation for the relaxation stress (Eq.3.10).

METHODS & MATERIALS

Experimental Data for Model Development

Modeling of the consolidation and relaxation stresses both depend on experimentally derived compressive stresses. During the procedure for producing the prototype composites as described in the previous chapter the compressive stresses were gathered for each combination of species and density. More specifically the load required to hold the press at the desired press schedule was monitored and recorded along with the time and thickness between press platens.

Consolidation Model – Experimental Methods

The compressive force and distance between platens acquired during the pressing of prototype panels was used in calculating the relationship between density and pressure of individual mats. Non-linear regression techniques (Marquardt-Levenberg method) were utilized to fit the variable K (Eq. 3.5) to the strand bending model, and to fit the compression modulus E_c (Eq.3.7) to the strand consolidation model. This process was completed for 6 panels of each species and density. K and E_c were averaged for each species and density.

The compressive force and time data in transient and asymptotic relaxation region (Figure 3.3) acquired during the pressing of prototype panels was used in calculating the relationship between time and pressure of individual mats. Relaxation time variables λ_1 , λ_2 , λ_3 , and λ_4 are set to e^1 , e^3 , e^5 , and e^7 (Eq. 3.10). Non-linear regression techniques (Marquardt-Levenberg method) were then used to fit the variables E_1 , E_2 , E_3 , and E_4 to the time pressure relationship. The process was completed for 6 panels of each species and density.

Pulling force Equation 3.6,8 and 10 were integrated using the Riemann integral, so that the accumulated pulling force could be analyzed. The elements were then summed to determine the total pulling force accumulated along the length of the pultrusion die.

Friction

The coefficient of friction associated with a strand composite pultrusion process was determined using testing procedures based on ASTM Standard D 2394 for wood veneers of radiata pine (*Pinus radiata*). The test used for two 63 mm by 102 mm veneers to be placed between 76 by 152 mm heated platen with a 63 mm by 102 mm pulling between the two test specimens. Virgin grade leather 10 mm thick was adhered to either side of the pulling block to create a non-slip surface. A screw driven universal testing machine was utilized to pull the pulling block and the specimens on either side of the pulling block along the surface of the heated platens at a rate of 76 mm per minute. A servo-hydraulic universal testing machine was utilized to apply a constant normal force to the heated platens. The frictional force used to pull the pulling block and the normal force applied

to the heated platens was used to calculate the static and dynamic coefficients of friction.

Figure 3.5 shows a diagram of the test procedure used. (Englund, 2001)

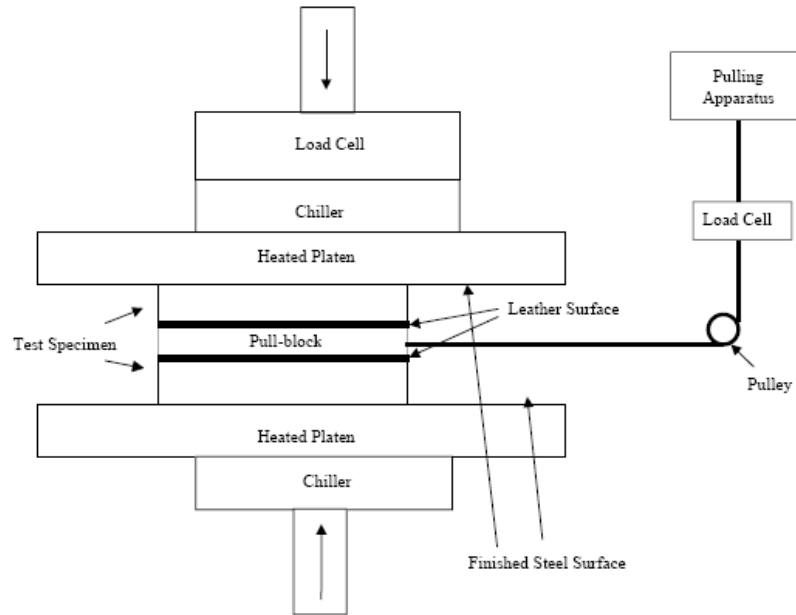


Figure 3.5 - Test procedure for determining coefficient of friction (Englund, 2001)

A range of platen temperatures, and normal loads were observed during the testing.

Platen temperatures were 150, 160, 170 degree Celsius. Normal loads were 35, 65, and 135 kN. Five specimens were tested for each set of normal loads, and temperatures.

Density Adjustment

The data from this research and from past literature shows that density of strand composites has a drastic effect on the tensile properties of strand composites (Meyers 2001, Wang and Lam 1999, Bozo 2002). In the case of strand composite pultrusion the limiting tensile capacity will generally correlate to the point with the lowest density.

Variation in density along the length of composites was measured in all tension specimens per target density and species after the tension testing was complete. Tension

coupons were cut into a series of 38 mm by 51 mm density specimens. The dimensions and weight of each density specimen were recorded and the density calculated.

Pultrusion

The pultrusion process (Figure 3.1) was constructed to test the feasibility of pultruding strand composites. A variable speed 177 mm wide conveyor belt aided the uncompressed strand mat into the pultrusion die. A pultrusion die fabricated for the process included a 362 mm long entrance section with a 12% taper, consolidating the composite to the final cross section of 13 mm by 102 mm and a 457 mm long constant geometry section. A series of ten polyurethane covered rollers driven by a variable speed motor compressed the composite on either side to pull the composite through the process. The pultrusion die is free-standing and floats on a series of roller, supported horizontally only by two load cells. The two 13.3 kN load cells were attached between the puller and the pultrusion die to measure the pulling forces developed during processing.

The production of wood strand pultruded composites for this research begins the same way as the production of the prototype panels discussed earlier. The resin is applied and the mats are formed using the same production methods used in Chapter 2. The mats are cut into four 76 mm wide strips of mat and the 89 mm on each side of the mat are discarded. The strips of mat are then connected end to end to form a continuous strand mat.

The pultrusion process is started using 2.44 m long sections of veneer. The use of veneers allows for a continuous link between the puller and the strand mat to get the

process started. Continuous prepreg carbon fiber reinforces the veneers and strand mat to increase tensile strength during the processing.

RESULTS & DISCUSSION

Consolidation Stress

A generalized mat consolidation model for wood composites (Zhou & Dai, 2008) was used to predict the consolidation stress of the composite. The low stress region (mat density < strand density) of the mat consolidation was described using a semi-empirical bending model and the high stress region (mat density > strand density) was described using a strand mat compression model developed by Dai & Steiner (1993).

In the generalized mat consolidation model (Dai & Zhou, 2008) the material type (i.e strand mat, fibrous mat, or particle mat) is accounted for in the exponent n . Theoretical derivations were used to establish a value of 5 for n for mats with 2-dimensional bending elements such as strand mats (Zhou & Dai, 2008).

The variable K is a combination of a constant value from the derivation of the 2-dimensional strand bending equation and a structural factor accounting for the variability in bending unit dimensions and the distance between bending units. Non-linear regression techniques (Marquardt-Levenberg method) were implemented to fit the variable K to the experimental compression data. The variable K for all combinations of species and density are shown in Table 3.1.

Table 3-1 - Parameters for compression stress modeling

Species	Target Density (kg/m³)	E_c (MPa)	K (*10⁻⁴)
Ponderosa Pine	560	17.44 (4.19)	1.24 (0.59)
	680	25.59 (3.08)	2.08 (0.46)
	800	22.53 (3.45)	1.45 (0.13)
	Average	21.85 (4.84)	1.59 (0.55)
Lodgepole Pine	560	22.21 (8.19)	2.00 (0.95)
	680	15.49 (1.72)	0.80 (0.28)
	800	23.19 (4.24)	1.67 (0.39)
	Average	20.30 (6.19)	1.49 (0.78)
Grand Fir	560	13.81 (2.72)	0.79 (0.25)
	680	11.36 (2.86)	0.57 (0.132)
	800	13.80 (1.46)	0.73 (0.11)
	Average	12.99 (2.57)	0.69 (0.19)

*Values in parenthesis denote standard deviation

Prediction of the high stress region was made utilizing a mat consolidation model by Dai & Steiner (1993). Inputs of strand dimensions, strand density and strand compression modulus E_c were employed to generate stress density relationships with the mat consolidation model for each species. Strand dimensions and strand densities were determined in Chapter 2. Utilizing non-linear regression techniques (Marquardt-Levenberg method) the compression modulus for each species was fit to the experimental data. Values for the compression modulus are shown in Table 3.1.

The strand bending model was used to predict stress below 400 kg/m³ and the compression model was used to predict stress above 400 kg/m³ as indicated in Zhou and Dai (2008) model prediction. The combination of the strand bending and compression models showed good fit to the experimental compression data, as shown in Figures 3.6 through 3.8.

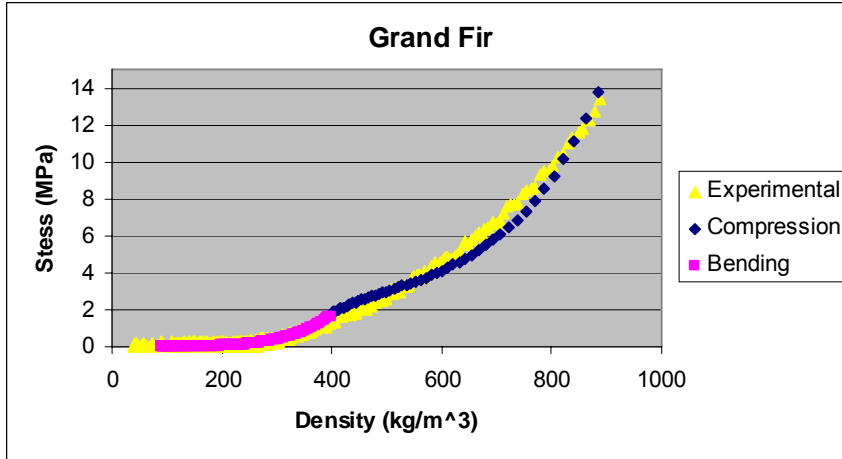


Figure 3.6 - Predicted & experimental consolidation stress for grand fir

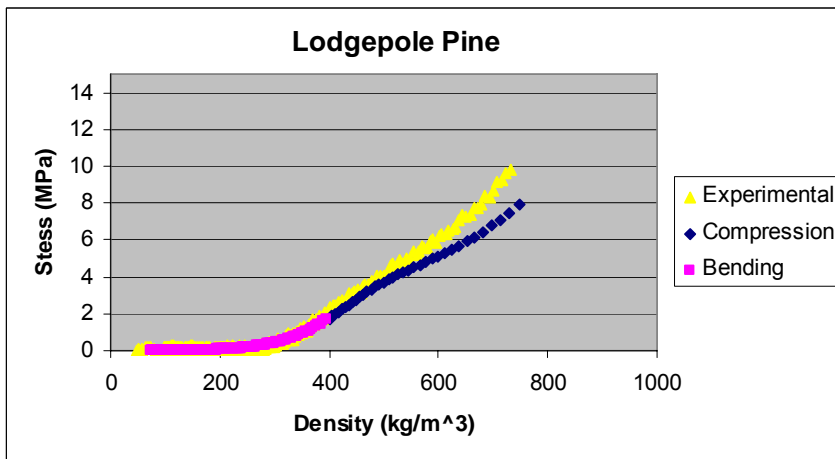


Figure 3.7 - Predicted & experimental consolidation stress for lodgepole pine

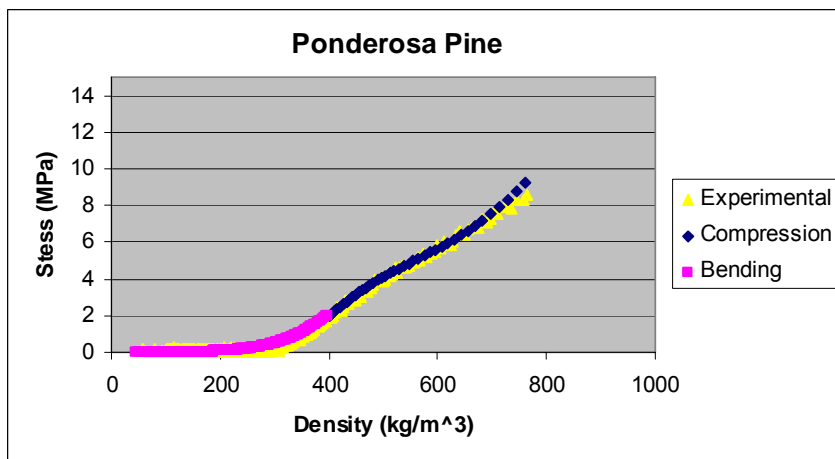


Figure 3.8 - Predicted & experimental consolidation stress for ponderosa pine

Relaxation Stress

A four parameter generalized Maxwell model was used to predict the relaxation stress of the composite. The modulus values E_1 , E_2 , E_3 , and E_4 in the Maxwell model were fit to experimental stress data using non-linear regression techniques (Marquard-Levenberg method) for each species and target density, as shown in Table 3.2.

Table 3-2 - Relaxation stress model parameters

Species	Target Density (kg/m ³)	E ₁ (MPa)	E ₂ (MPa)	E ₃ (MPa)	E ₄ (MPa)
Ponderosa Pine	560	1.72 (0.32)	3.30 (0.36)	1.47 (0.21)	1.45 (0.24)
	680	2.66 (0.60)	3.81 (0.55)	1.15 (0.58)	2.86 (0.52)
	800	4.76 (0.22)	5.41 (0.99)	2.23 (0.92)	2.93 (0.54)
	Average	2.71 (1.30)	3.93 (1.00)	1.55 (0.64)	2.26 (0.76)
Lodgepole Pine	560	2.04 (1.03)	3.08 (0.64)	1.11 (0.38)	1.48 (0.28)
	680	4.94 (4.35)	3.54 (0.74)	1.25 (0.70)	1.58 (0.39)
	800	2.93 (1.45)	5.74 (2.04)	1.90 (0.78)	2.46 (0.19)
	Average	2.69 (1.66)	3.81 (1.30)	1.31 (0.59)	1.70 (0.44)
Grand Fir	560	1.87 (0.73)	3.11 (0.31)	1.40 (0.27)	1.42 (0.25)
	680	3.03 (1.64)	3.24 (0.65)	1.07 (0.16)	1.32 (0.49)
	800	4.01 (1.85)	7.46 (2.80)	2.63 (0.86)	4.64 (1.94)
	Average	2.89 (1.57)	4.25 (2.32)	1.57 (0.77)	2.18 (1.73)

*Values in parenthesis denote standard deviation

The Maxwell model provided an accurate prediction of the relaxation stresses associated with the compression of strand composites. The low precision of the experimental compressive stress data was caused by the small size of the strand mat compared to the size of the press and will cause some error in the final model predictions. Figure 3.9 and 3.10 show examples of the experimental and predicted relaxation response.

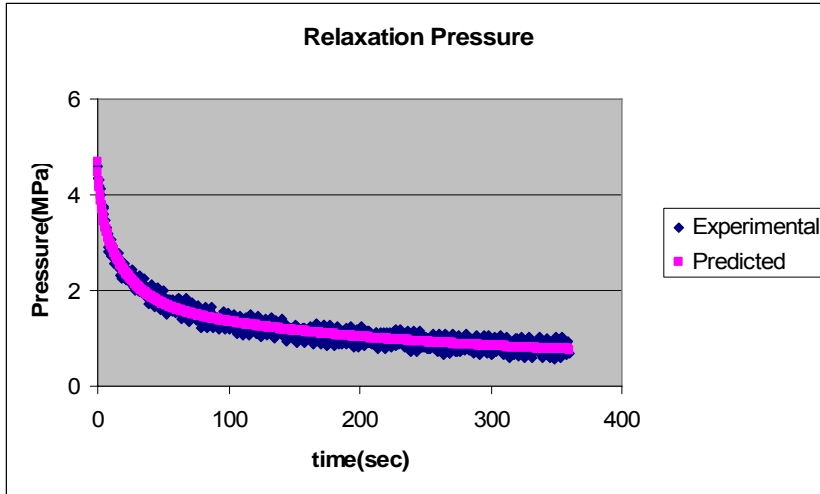


Figure 3.9 - Relaxation stress for ponderosa pine mat compressed to 560 kg/m³

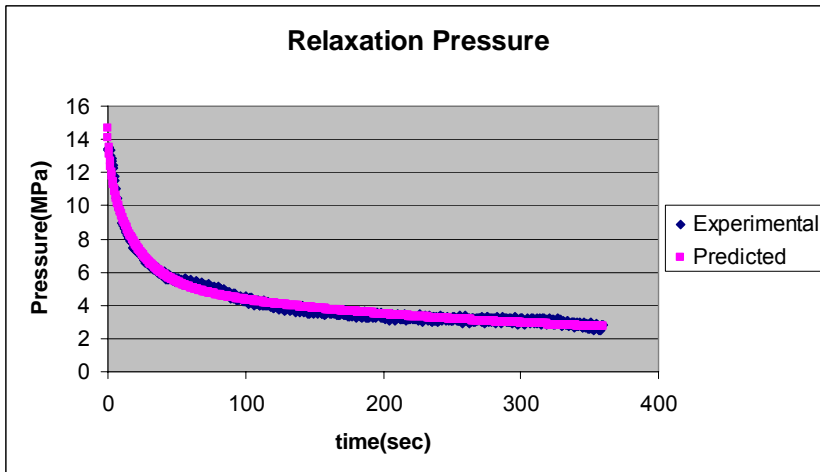


Figure 3.10 -Relaxation stress for grand fir strand mat compressed to 800 kg/m³

Friction Coefficient

Temperature and normal stress were tested to determine their influence on the dynamic and static coefficients of friction. GLM procedure and Duncan testing showed temperature had a significant influence on the coefficient of friction, and normal force had no influence on the coefficient of friction. Figure 3.11 shows the dynamic and static frictional coefficients with respect to temperature. A value of 0.08 was identified as the coefficient of friction for this research based on the temperature in the pultrusion die.

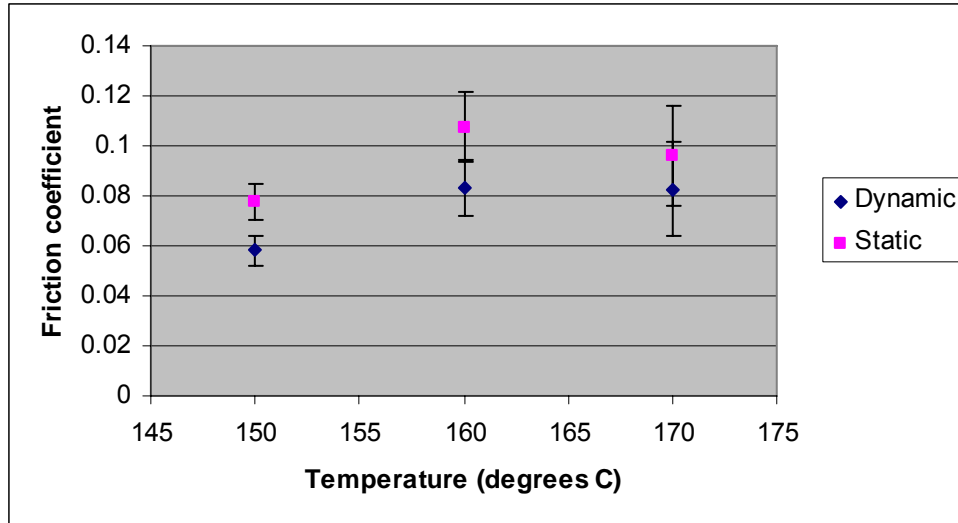


Figure 3.11 - Dynamic & static frictional coefficients with temperature

Pulling Force Model

The pulling force model was used to predict the accumulated force developed in the pultrusion die. Table 3.3 shows the total accumulated pulling force along with the force due to normal force in the entrance section, frictional force in the entrance section, and frictional force in the constant geometry section using Equation 3.1.

Table 3-3 - Calculated pulling force

Species	Target Density (kg/m ³)	Consolidation (kN)	Friction		Total (kN)
			Entrance (kN)	CG (kN)	
PP	560	1.04	0.70	3.25	8.94
	680	1.24	0.84	5.32	13.56
	800	2.34	1.58	6.84	19.19
LP	560	0.65	0.44	2.95	7.41
	680	1.54	1.04	3.32	10.26
	800	1.69	1.14	5.64	15.25
GF	560	0.77	0.55	3.39	8.65
	680	0.93	0.63	2.87	7.93
	800	2.35	1.59	10.19	25.91

Figures 3.12 through 3.14 graph the pulling forces from Table 3.3 and the ultimate strength values from Chapter 2 with density. The average ultimate strength values exceed their corresponding pulling forces for all species. The design ultimate strength values show varying success of exceeding the pulling force. The large variation in design ultimate strength values can be attributed to low confidence due to the small sample size and therefore may not be very accurate.

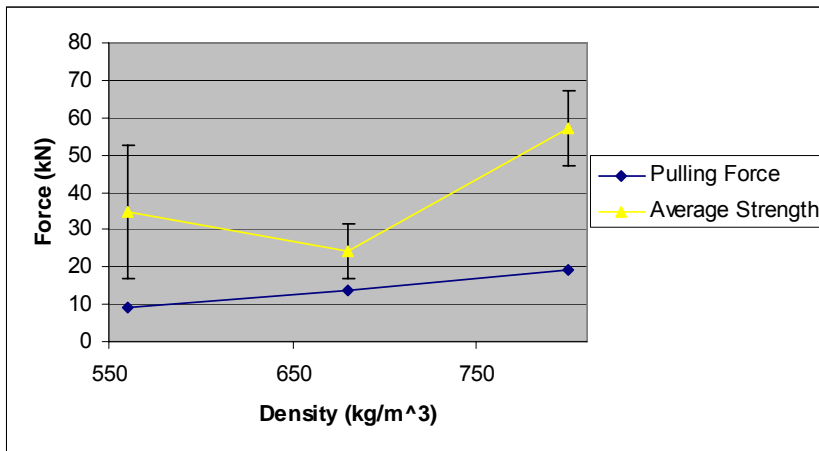


Figure 3.12 - Comparison of pulling force and ultimate tensile strength for ponderosa pine

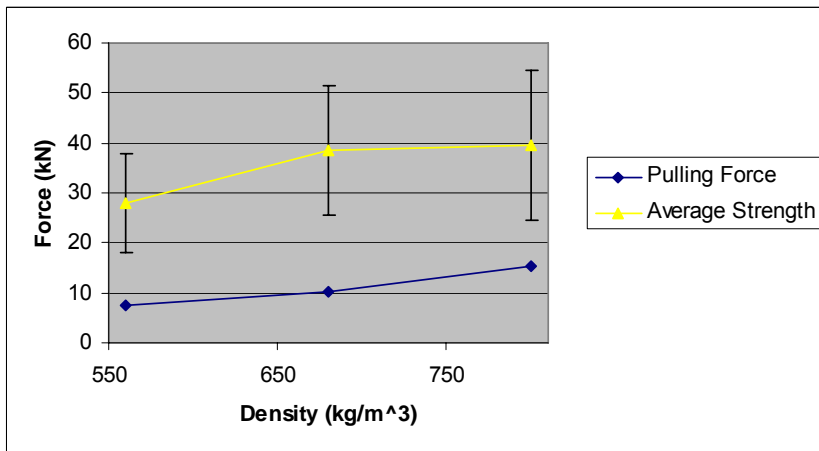


Figure 3.13 - Comparison of pulling force and ultimate tensile strength for lodgepole pine

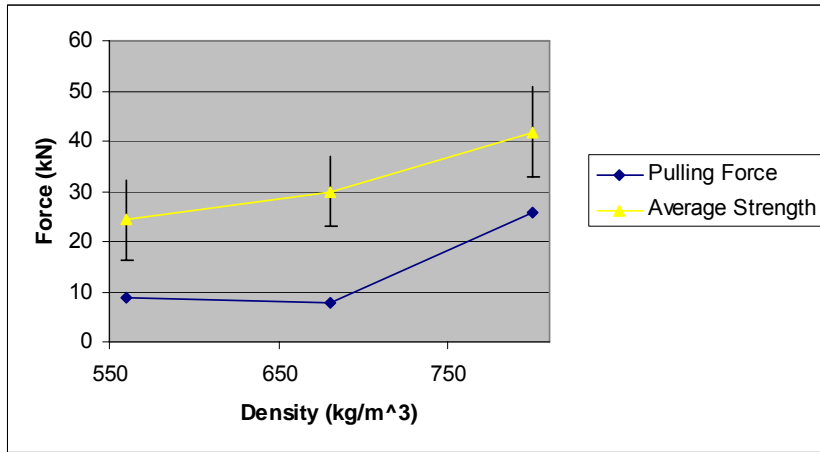


Figure 3.14 -Comparison of pulling force and ultimate tensile strength for grand fir

By developing the pulling force model as an integral allows for the calculation of the accumulated pulling force along the length of the pultrusion die. Figure 3.15 shows the accumulated pulling force of ponderosa pine for three target densities. Figures of the accumulated pulling force for grand fir and lodgepole pine showed similar trends and can be viewed in the Appendix F. The accumulated pulling force is less than 30% of total accumulated stress at the end of the tapered section and less than 0.1% of the total accumulated stress half way through the tapered section. Such low accumulated pulling forces early in the pultrusion process suggest that the ultimate tensile strength of the strand composite prior to the complete cure of the resin should still exceed the accumulated pulling force.

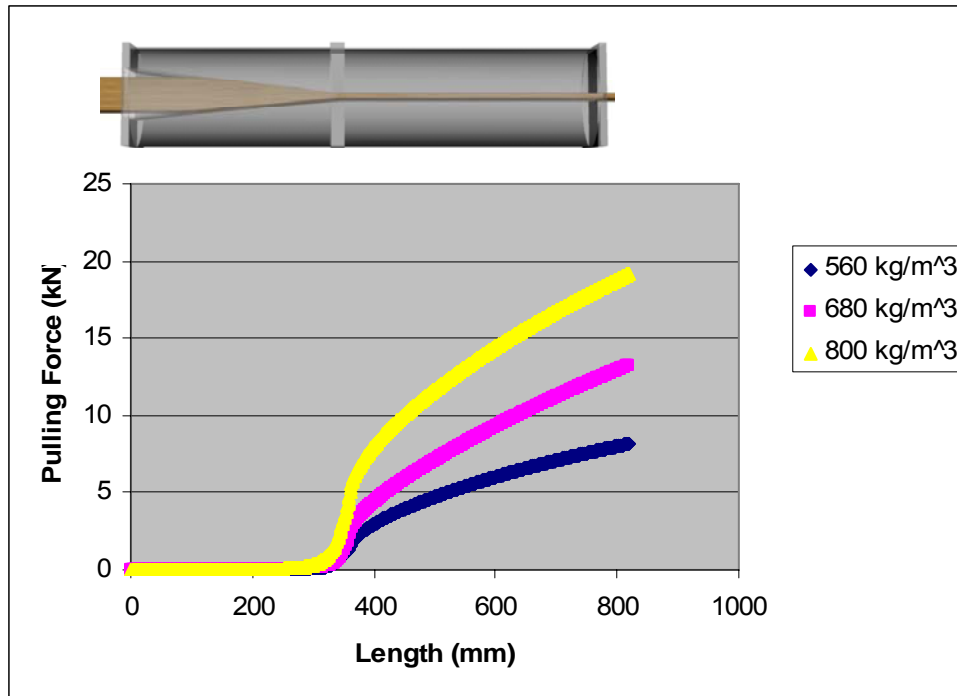


Figure 3.15 - Accumulated pulling force for ponderosa pine

Optimization of Entrance Angle

The taper of the entrance section may influence forces developed in the entrance section of the pultrusion die. The pulling force model was used to determine the optimum entrance angle in the entrance section. The experimental data used to calculate the change in pulling force with entrance angle was collected during the pressing of prototype panels with a press schedule corresponding to a taper of 12%. Figure 3.16 shows the predicted total pulling force, frictional force, and normal force in the tapered section of the die with varying entrance angle. The normal force shows little variation with increase in entrance angle compared to the influence of entrance angle on frictional force. The large decrease in frictional force with increasing entrance angle can be related to the decrease in contact area between the strand composite and the pultrusion die as entrance angle is increased.

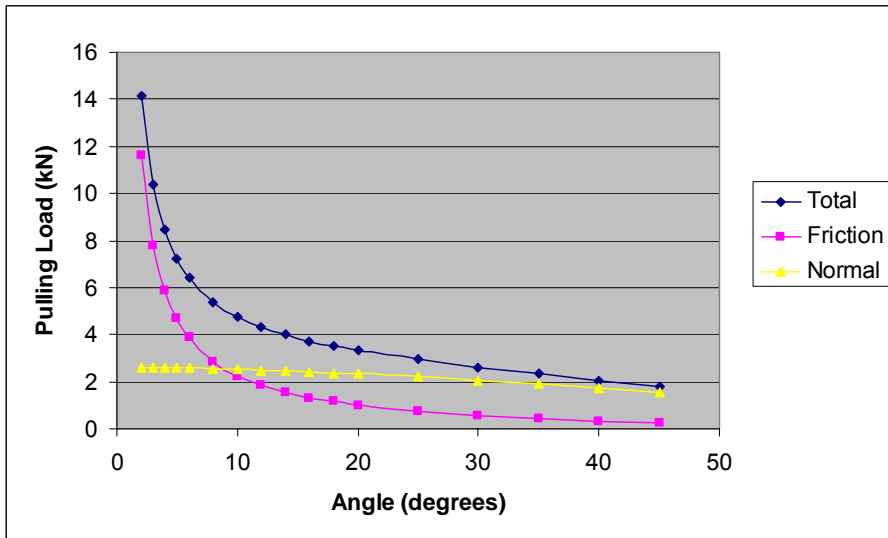


Figure 3.16- Pulling force in entrance section with varying entrance angles

Friction Sensitivity

Figure 3.11 shows that the frictional coefficient could range from as low as 0.052 to 0.12. Due to the wide range of frictional coefficients a sensitivity analysis was conducted to determine the influence of the frictional coefficient of the pulling force model. Table 3.4 shows the pulling force with extreme frictional coefficients for all species and target densities. The pulling force model is quite sensitive to friction pulling forces for all species and density.

Table 3-4- Pulling forces for extreme friction coefficients

Species	Target Density (kg/m ³)	$\mu=0.052$ (kN)	$M=0.12$ (kN)
Grand Fir	560	5.89	12.59
	680	5.48	11.42
	800	17.66	37.69
Lodgepole Pine	560	5.05	10.80
	680	7.21	14.63
	800	10.50	22.03
Ponderosa Pine	560	6.17	12.89
	680	9.25	19.72
	800	13.29	27.61

Density Variation

The data from this research and from past literature (Meyer, 2001, Wang & Lam 1999) shows that density of strand composites has a drastic influence on the tensile properties of strand composites and can vary significantly throughout a strand composite(Bozo, 2002). Large variations in density will correspond to sections of composite with reduced tensile strength. Therefore if there are large variations in density along a composite the ultimate tensile capacity of the composite could drop below the required pulling force causing failure of the composite within the pultrusion die.

A rather significant amount of variation in density was found in each panel. On average variation in density along the panel length was 10.23% of the average panel density.

There was little difference in variation of density along a panel between species.

However, the variation in density along a panel did decrease with increasing density.

Figure 3.17 shows the variation in density along a panel at different average densities and for different species.

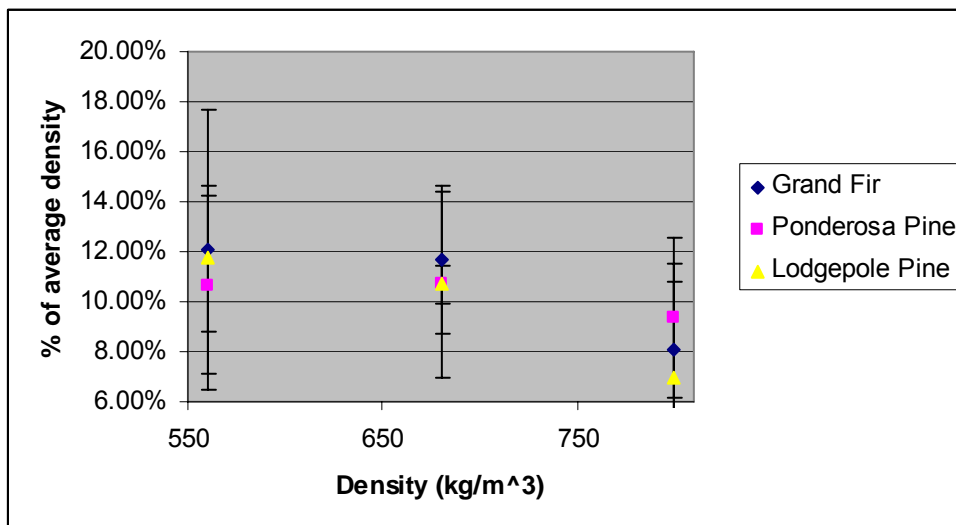


Figure 3.17- Density variation in prototype panels

Pultrusion of Wood Strand Composites

The success of the strand composite pultrusion process is dependent on the tensile capacity of the composite exceeding the pulling force developed in the pultrusion die. Figures 3.12 through 3.14 show that the average ultimate tensile strength of the composite and the predicted pulling force with respect to density. From Figures 3.12 through 3.14 it is reasonable to assume that a pultrusion process is possible for composite densities above 560 kg/m^3 . The pultrusion process constructed for this research was equipped with two 13.3 kN load cells, setting the upper limit for processing below 26.6 kN. The pulling force model predicts that a load of 26.6 kN corresponds to a composite density near 720 kg/m^3 for each species. When processing was attempted it was discovered that the pulling motor was actually the limiting factor lowering the upper limit to less than 22.2 kN and the maximum density to 670 kg/m^3 .

Problems arose when attempting to bridge the strand composite to the pulling motor to initiate processing. A set of four veneers were used to bridge the composite to the strand mat. Veneers were overlaid on the top and bottom of the strand mat for a short distance in order to transfer the load from the veneers to the strand mat. Preperg carbon fiber was also used add tensile strength to the composite. The density on the short length of strand mat with overlain veneers was reduced by removing strands based on the uncompressed mat height. Controlling the density in the short length of strand mat with overlain veneers proved difficult and inconsistent. If the density was too low the force would not transfer from the veneers to the strand mat and the composite would fail in the pultrusion die. If the density was too high the pulling force would exceed the limits of the

pultrusion process and the puller would break. Starting the pultrusion process was attempted numerous times. Variation in composite thickness, resin content, strand type, and various carbon fiber reinforcement configurations were attempted with little success.

CONCLUSION

Uni-directional strand mats were produced using flat press techniques to simulate conditions in the pultrusion die. During pressing experimental compressive stresses were recorded for a range of densities and species. Large variations in the experimental compressive stresses due to precision of load cells on the flat press equipment were observed. Models for the consolidation stress due to bending of individual strands, compression of stand mats and relaxation stresses of uni-directional strand mats showed good fit with experimental data. All stresses were within the range of the error due to the precision of the load cells.

Dynamic and static coefficients of friction were determined for varying temperatures, and normal forces. Normal force showed no significant influence on the coefficient of friction. An average coefficient of friction 0.08 was used in the modeling of the pulling force. A range of possible frictional coefficients for a pultrusion process of 0.052 to 0.12 was determined and applied to the pulling force model to determine the model sensitivity to friction.

A solid mechanics based model was developed to predict the pulling force within the pultrusion die. Integrals of the frictional and normal forces associated with consolidation

of strand mats were utilized to determine the accumulation of pulling force along the length of the pultrusion die. The pulling force was calculated for a range of densities and species and compared to the tensile strength of the composite to determine the feasibility of the strand composite pultrusion process and are shown in Figures 3.12 through 3.14. The average tensile strength of composites of all species with densities above 560 kg/m³ exceeded their associated pulling force.

The influence of entrance angle on pulling force was analyzed using the pulling force model. Figure 3.16 shows that as the entrance angle increased pulling force in the entrance section decreases. Much larger decreases were observed for the frictional component than for the normal component of the pulling force.

A pultrusion process was developed and constructed. However, mechanical restraints and difficult starting procedures did not allow for the production of any pultruded strand composites.

REFERENCES

- ASTM D2394 -05e1 Standard Test Methods for Simulated Service Testing of Wood and Wood - Base Finish Flooring.* American Society for Testing and Materials, 2005.
- Bozo, Alejandro M. "Spatial Variation of Wood Composites." Aug 2002. Thesis. Washington State University.
- Christensen, R.M. *Theory of Viscoelasticity, An Introduction.* New York and London: Academic Press, 1971.

- Dai, Chunping, and Paul R. Steiner. "Compression behavior of randomly formed wood flake mats." *Wood and Fiber Science* 25.4 (1993): 349-358.
- Englund, Karl. "Consolidation and friction mechanisms of wood composites and their influence on pultrusion processing." Dec 2001: all. Thesis. Washington State University.
- Lang, Elemer M., and Michael P. Wolcott. "A model for viscoelastic consolidation of wood strand mat. Part II: static stress-strain behavior of the mat." *Wood and Fiber Science* 28.3 (1996): 369-379.
- Lenth, Christopher A., and Fredrick A. Kamke. "Investigation of flakeboard mat consolidation Part II. Modeling mat consolidation using theories of cellular materials." *Wood and Fiber Science* 28.3 (1996): 309-319.
- Malvern, Lawrence E. *Introduction to the mechanics of a continuous medium*. Englewood Cliffs, NJ: Prentice-Hall, Inc., 1969.
- Meyers, Kristin Lynne. "Impact of strand geometry and orientation on mechanical properties of strand composites." Dec 2001: 22-43. Thesis. Washington State University.
- Wang, Kaiyuan, and Frank Lam. "Quadratic RSM models of processing parameters for three-layer oriented flakeboard." *Wood and Fiber Science* 31.2 (1999): 173-186.
- Wolcott, Michael P., Fredrick A. Kamke, and D.A. Dillard. "Fundamentals of flakeboard manufacture: viscoelastic behavior of the wood component." *Forest Products Journal* 22.4 (1990).

Zhou, Cheng, Chunping Dai, and Gregory D Smith. "A generalized mat consolidation model for wood composites." *HOLZFORSCHUNG* 62.2 (2008): 201-208.

CHAPTER 4 : PROJECT SUMMARY & CONCLUSIONS

The success of a strand composite pultrusion process is dependent on the tensile capacity of the strand composite exceeding the accumulated pulling force developed in the pultrusion die. The accumulated pulling force was modeled based on the compressive behavior of prototype strand composites and the physical characteristics of the pultrusion die. Strand and strand mat properties were analyzed to determine if small diameter timbers would make a reliable material source for a strand composite pultrusion process. The average ultimate tensile strengths of strand composites made from small diameter timbers exceeded the predictions from the pulling force model suggesting that a strand pultrusion process is feasible.

Small Diameter Timbers in Long Strand Composites

Strand and strand composite physical and mechanical properties were summarized. Tests were performed to calculate the tension modulus of individual strand and strand composites at a range of densities. Physical properties of strands were measured including dimensions, specific gravity, grain angle, and strand processing recovery.

The results of the mechanical and physical testing of individual strand and strand composites showed dependence of most parameters on species. Strand dimensions all showed some significant differences between species, except for strand thickness. Strand grain angle was unusually well aligned when compared to previous research (Yadama 2002, Langum 2006). Species was shown to have significant influence on the grain

angle. Tension properties of individual strands showed a dependence on both density and species. Ultimate tensile strength of strand composites showed a significant influence of density and species, while tensile modulus showed a significant dependence on target density and species. Processing recovery data showed that Grand fir yields a much smaller amount of usable strands than Lodgepole and Ponderosa pine.

Pulling Force Model

The feasibility of a strand pultrusion process was determined by developing a pulling force model that incorporates the compressive behavior of strand mats and the geometry of the pultrusion die. Models for the consolidation stress due to bending of individual strands, compression of stand mats and relaxation stresses of uni-directional strand mats showed good fit with experimental data. All stresses were within the range of the inherit error due to the precision of the load cells during pressing of prototype panels.

Dynamic and static coefficients of friction were determined for varying temperatures, and normal forces. Statistical analyses determined that temperature significantly influences the coefficient of friction and not normal force. A range of possible frictional coefficients for a pultrusion process were determined and applied to the pulling force model to determine the model sensitivity to friction.

The pulling force was calculated for a range of densities and species and compared to the tensile strength of the composites to determine the feasibility of the strand composite pultrusion process. The average tensile strength of composites of all species with densities above 560 kg/m^3 exceeded their associated pulling force.

Predictions of the accumulated pulling force along the length of the pultrusion die showed that on less than 30% of the accumulated pulling force was developed by the end of the tapered section and less 0.1% of the accumulated pulling force was developed half way through the tapered section. This suggests that even though the strand composite has not been allowed to fully cure the strand composite may still be capable of withstanding the tensile capacity at that point in the process. Density variations throughout the prototype panels varied between + or – 10.23% and could attribute to lower tensile capacities in the strand composite during pultrusion.

Pultrusion Process

A pultrusion process was developed and constructed. The pultrusion process consisted of: A conveyor belt that would feed the uncompressed strand mat into the pultrusion die. The pultrusion die with a tapered entrance section and constant geometry section consolidated the strand mat the final dimensions and allowed for resin to cure. Load cells measured the pulling force. A pulling mechanism drove the pultrusion process.

However, mechanical restraints and difficult starting procedures did not allow for the production of any pultruded strand composites. With increased capacity in the pulling mechanism it is highly possible that strand composites could be produced with a pultrusion process. The pultrusion process did not produce any strand composites, but veneer composites were produced with great ease and the pulling forces associated with there production were quite low.

APPENDIX A– GLM PROCEDURE & DUNCAN TEST FOR STRAND DIMENSIONS

GLM for Zachs Strand Dimension 11:20 Tuesday, July 1, 2008 19

The GLM Procedure

Class Level Information

Class	Levels	Values
Species	3	GF LP PP

Number of Observations Read	360
Number of Observations Used	360

GLM for Zachs Strand Dimension 11:20 Tuesday, July 1, 2008 20

The GLM Procedure

Dependent Variable: Length Length

Source	DF	Sum of Squares	Mean Square	F Value	Pr > F
Model	2	80.833263	40.416631	9.97	<.0001
Error	357	1447.656274	4.055060		
Corrected Total	359	1528.489537			

R-Square	Coeff Var	Root MSE	Length Mean
0.052884	19.09258	2.013718	10.54713

Source	DF	Type I SS	Mean Square	F Value	Pr > F
Species	2	80.83326292	40.41663146	9.97	<.0001

Source	DF	Type III SS	Mean Square	F Value	Pr > F
Species	2	80.83326292	40.41663146	9.97	<.0001

The GLM Procedure

Dependent Variable: Width Width

Source	DF	Sum of Squares	Mean Square	F Value	Pr > F
Model	2	20.1653727	10.0826863	33.92	<.0001
Error	357	106.1289779	0.2972801		
Corrected Total	359	126.2943505			

R-Square	Coeff Var	Root MSE	Width Mean
0.159670	61.89256	0.545234	0.880936

Source	DF	Type I SS	Mean Square	F Value	Pr > F
Species	2	20.16537267	10.08268634	33.92	<.0001

Source	DF	Type III SS	Mean Square	F Value	Pr > F
Species	2	20.16537267	10.08268634	33.92	<.0001

The GLM Procedure

Dependent Variable: Thickness Thickness

Source	DF	Sum of Squares	Mean Square	F Value	Pr > F
Model	2	0.00035328	0.00017664	0.62	0.5411
Error	357	0.10249120	0.00028709		
Corrected Total	359	0.10284448			

R-Square	Coeff Var	Root MSE	Thickness Mean
0.003435	55.38677	0.016944	0.030592

Source	DF	Type I SS	Mean Square	F Value	Pr > F
Species	2	0.00035328	0.00017664	0.62	0.5411

Source	DF	Type III SS	Mean Square	F Value	Pr > F
Species	2	0.00035328	0.00017664	0.62	0.5411

The GLM Procedure

Dependent Variable: Slenderness Slenderness

Source	DF	Sum of Squares	Mean Square	F Value	Pr > F
Model	2	151233.368	75616.684	6.69	0.0014
Error	357	4034388.530	11300.808		
Corrected Total	359	4185621.898			

R-Square	Coeff Var	Root MSE	Slenderness Mean
0.036132	28.68576	106.3053	370.5855

Source	DF	Type I SS	Mean Square	F Value	Pr > F
Species	2	151233.3680	75616.6840	6.69	0.0014

Source	DF	Type III SS	Mean Square	F Value	Pr > F
Species	2	151233.3680	75616.6840	6.69	0.0014

The GLM Procedure

Duncan's Multiple Range Test for Length

This test controls the Type I comparisonwise error rate, not the experimentwise error rate.

Alpha	0.05
Error Degrees of Freedom	357
Error Mean Square	4.05506

Number of Means	2	3
Critical Range	.5113	.5382

Means with the same letter are not significantly different.

Duncan Grouping	Mean	N	Species
A	11.1384	120	PP
B	10.5246	120	LP
C	9.9784	120	GF

The GLM Procedure

Duncan's Multiple Range Test for Width

This test controls the Type I comparisonwise error rate, not the experimentwise error rate.

Alpha	0.05
Error Degrees of Freedom	357
Error Mean Square	0.29728

Number of Means	2	3
Critical Range	.1384	.1457

Means with the same letter are not significantly different.

Duncan Grouping	Mean	N	Species
A	1.07592	120	PP
A	1.01905	120	LP
B	0.54784	120	GF

The GLM Procedure

Duncan's Multiple Range Test for Thickness

This test controls the Type I comparisonwise error rate, not the experimentwise error rate.

Alpha	0.05
Error Degrees of Freedom	357
Error Mean Square	0.000287

Number of Means	2	3
Critical Range	.004302	.004529

Means with the same letter are not significantly different.

Duncan Grouping	Mean	N	Species
A	0.031850	120	PP
A			
A	0.030496	120	GF
A			
A	0.029429	120	LP

The GLM Procedure

Duncan's Multiple Range Test for Slenderness

This test controls the Type I comparisonwise error rate, not the experimentwise error rate.

Alpha	0.05
Error Degrees of Freedom	357
Error Mean Square	11300.81

Number of Means	2	3
Critical Range	26.99	28.41

Means with the same letter are not significantly different.

Duncan Grouping	Mean	N	Species
A	391.59	120	PP
A			
A	377.38	120	LP
B	342.78	120	GF

APPENDIX B - CUMULATIVE FREQUENCY PLOTS OF STRAND DIMENSIONS

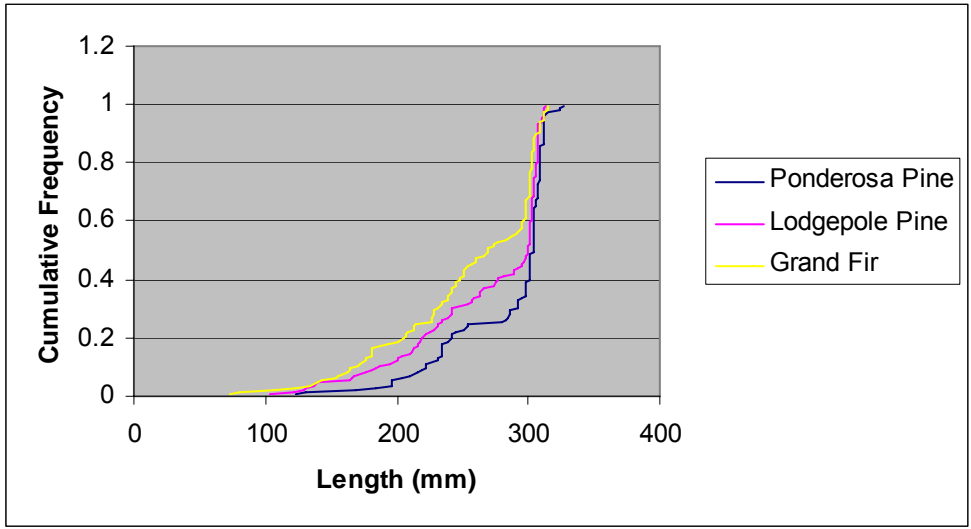


Figure B.1-Cumulative frequency plot for strand length

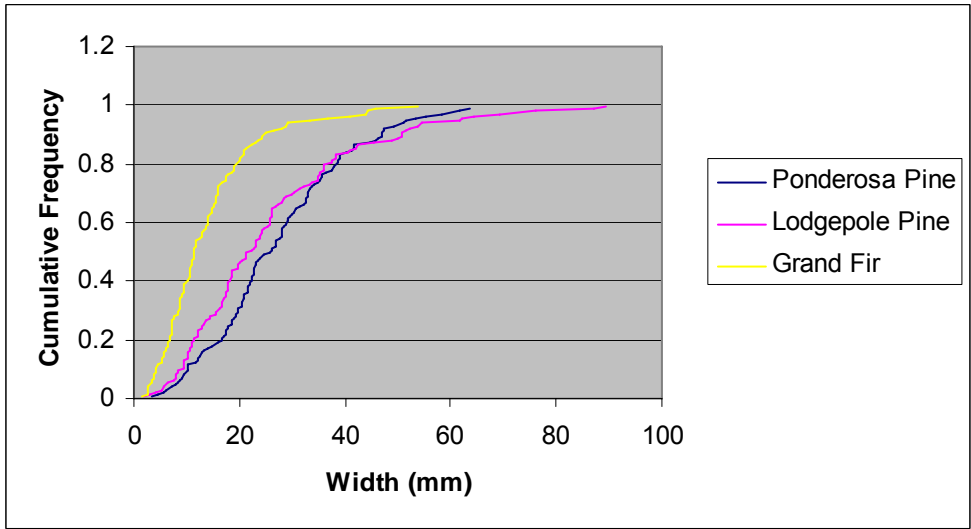


Figure B.2 - Cumulative frequency plot for strand width

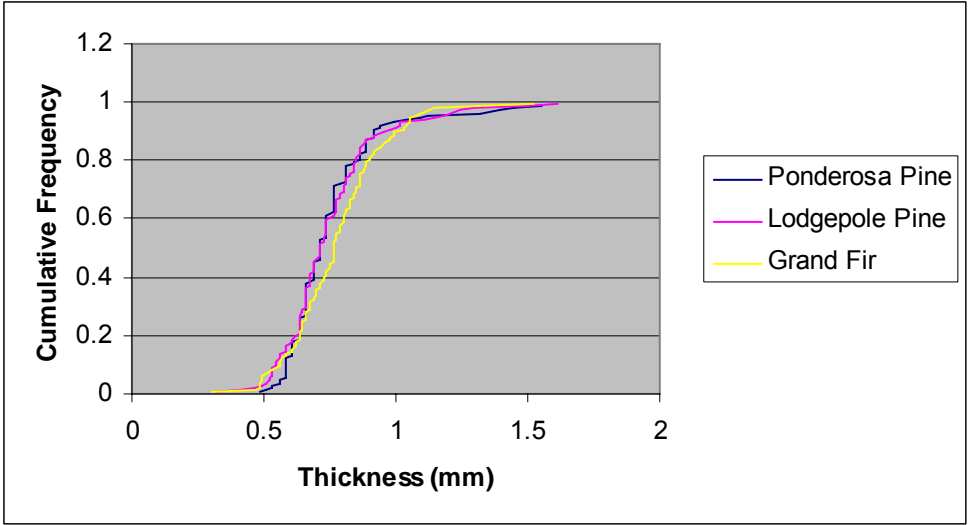


Figure B.3 - Cumulative frequency plot for strand thickness

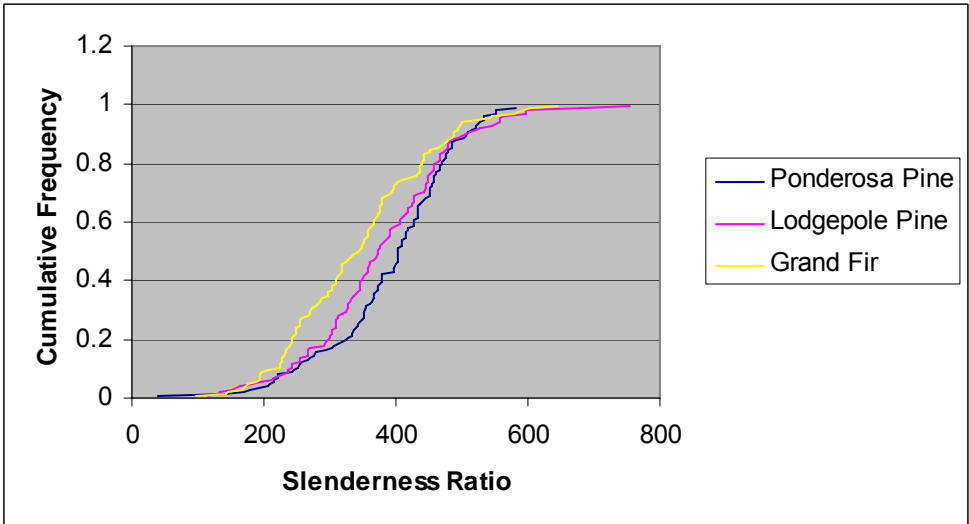


Figure B.4 - Cumulative frequency plot for strand slenderness ratio

APPENDIX C- GLM PROCEDURE & DUNCAN TEST FOR GRAIN ANGLE

GLM for Zachs Strands 08:46 Monday, June 23, 2008 64

The GLM Procedure

Class Level Information

Class	Levels	Values
Species	3	GF LP PP
Number of Observations Read		240
Number of Observations Used		240

GLM for Zachs Strands 08:46 Monday, June 23, 2008 65

The GLM Procedure

Dependent Variable: Grainangle Grainangle

Source	DF	Sum of Squares	Mean Square	F Value	Pr > F
Model	3	10.1184267	3.3728089	2.42	0.0669
Error	236	329.0761983	1.3943907		
Corrected Total	239	339.1946250			

R-Square	Coeff Var	Root MSE	Grainangle Mean
0.029831	92.52444	1.180843	1.276250

Source	DF	Type I SS	Mean Square	F Value	Pr > F
Species	2	8.32900000	4.16450000	2.99	0.0524
SpecificGravity	1	1.78942675	1.78942675	1.28	0.2584

Source	DF	Type III SS	Mean Square	F Value	Pr > F
Species	2	10.07071174	5.03535587	3.61	0.0285
SpecificGravity	1	1.78942675	1.78942675	1.28	0.2584

The GLM Procedure

Duncan's Multiple Range Test for Grainangle

This test controls the Type I comparisonwise error rate, not the experimentwise error rate.

Alpha	0.05
Error Degrees of Freedom	236
Error Mean Square	1.394391

Number of Means	2	3
Critical Range	.3678	.3872

Means with the same letter are not significantly different.

Duncan Grouping	Mean	N	Species
A	1.5138	80	PP
A			
B A	1.2563	80	LP
B			
B	1.0588	80	GF

APPENDIX D - GLM PROCEDURE & DUNCAN TEST FOR STRAND TENSILE PROPERTIES

GLM for Zachs Strands 08:46 Monday, June 23, 2008 64

The GLM Procedure

Class Level Information

Class	Levels	Values
Species	3	GF LP PP

Number of Observations Read	240
Number of Observations Used	240

GLM for Zachs Strands 08:46 Monday, June 23, 2008 66

The GLM Procedure

Dependent Variable: E E

Source	DF	Sum of Squares	Mean Square	F Value	Pr > F
Model	3	8.5476466E12	2.8492155E12	55.99	<.0001
Error	236	1.2009848E13	50889186078		
Corrected Total	239	2.0557495E13			

R-Square	Coeff Var	Root MSE	E Mean
0.415792	19.22998	225586.3	1173097

Source	DF	Type I SS	Mean Square	F Value	Pr > F
Species	2	1.0424805E12	521240246298	10.24	<.0001
SpecificGravity	1	7.5051661E12	7.5051661E12	147.48	<.0001

Source	DF	Type III SS	Mean Square	F Value	Pr > F
Species	2	4.3876323E12	2.1938161E12	43.11	<.0001
SpecificGravity	1	7.5051661E12	7.5051661E12	147.48	<.0001

The GLM Procedure

Dependent Variable: UTS UTS

Source	DF	Sum of Squares	Mean Square	F Value	Pr > F
Model	3	258434663	86144888	24.61	<.0001
Error	236	826133747	3500567		
Corrected Total	239	1084568409			

R-Square	Coeff Var	Root MSE	UTS Mean
0.238283	32.46838	1870.980	5762.469

Source	DF	Type I SS	Mean Square	F Value	Pr > F
Species	2	53325451.3	26662725.7	7.62	0.0006
SpecificGravity	1	205109211.3	205109211.3	58.59	<.0001

Source	DF	Type III SS	Mean Square	F Value	Pr > F
Species	2	155507223.0	77753611.5	22.21	<.0001
SpecificGravity	1	205109211.3	205109211.3	58.59	<.0001

The GLM Procedure

Duncan's Multiple Range Test for UTS

This test controls the Type I comparisonwise error rate, not the experimentwise error rate.

Alpha	0.05
Error Degrees of Freedom	236
Error Mean Square	3500567

Number of Means	2	3
Critical Range	582.8	613.5

Means with the same letter are not significantly different.

Duncan Grouping	Mean	N	Species
A	6276.3	80	GF
A			
A	5873.4	80	PP
B	5137.8	80	LP

APPENDIX E- STRAND COMPOSITE TENSILE PROPERTIES & DENSITY RELATIONSHIPS

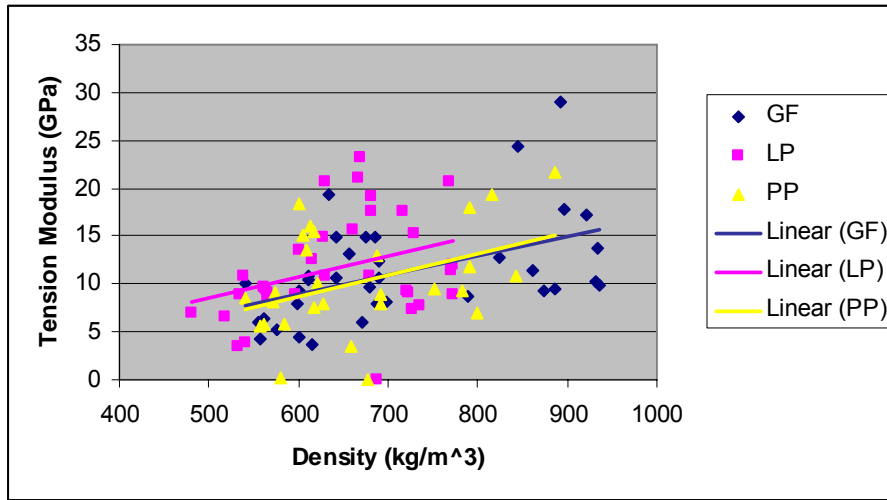


Figure E.1 – Strand composite tension modulus with density

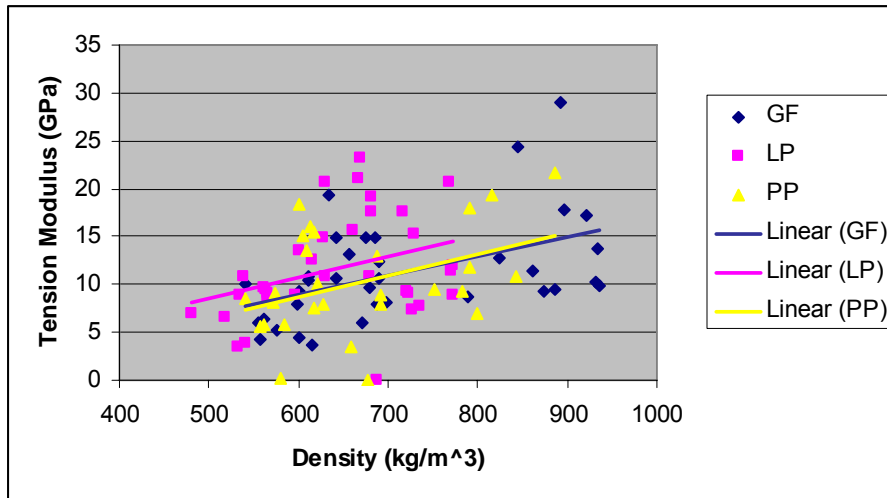


Figure E.2– Strand composite ultimate tensile strength with density

Table 4-1 – R² values for linear regression curves in Figures G.1 & G.2

Species	Tension Modulus	Ultimate Tensile Strength
Grand Fir	0.238	0.604
Lodgepole Pine	0.119	0.311
Ponderosa Pine	0.164	0.665

APPENDIX F- ACCUMULATED PULLING FORCE ALONG LENGTH OF PULTRUSION DIE

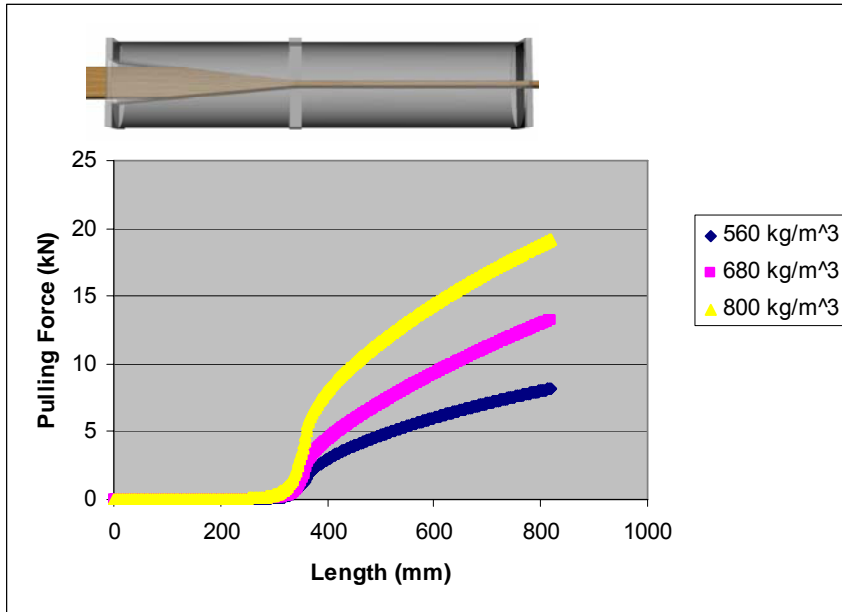


Figure F.1- Accumulated pulling force along pultrusion die for ponderosa pine

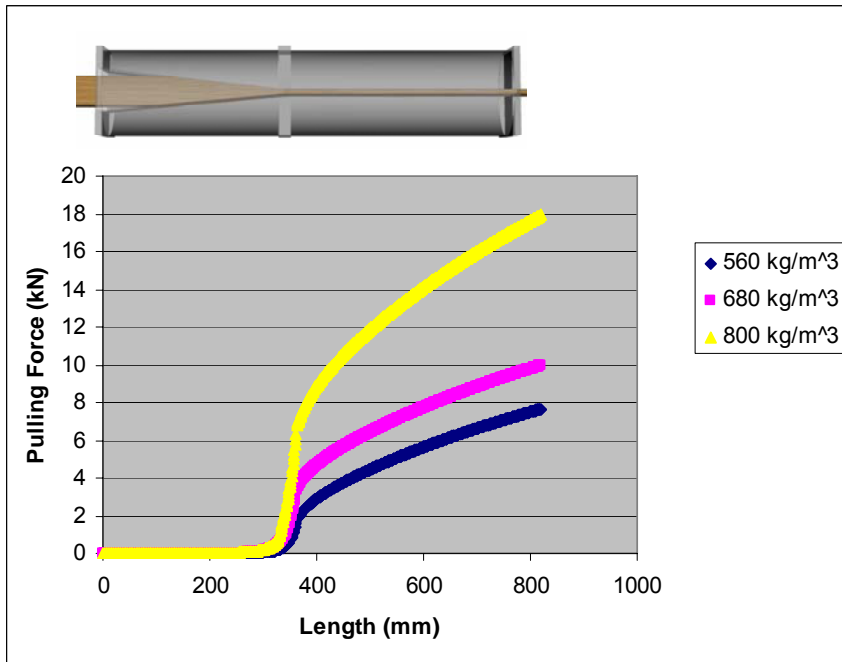


Figure F.2- Accumulated pulling force along pultrusion die for lodgepole pine

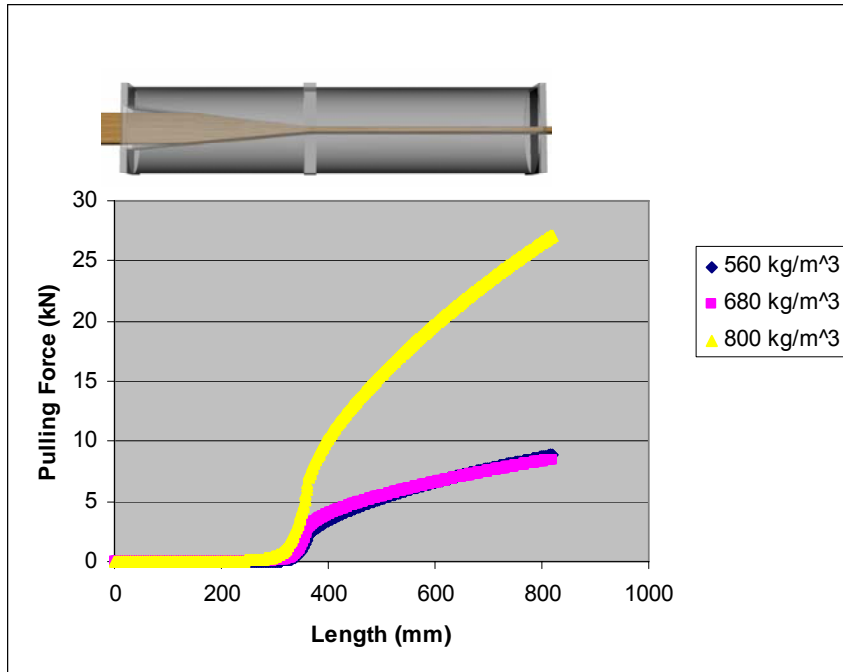


Figure F.3- Accumulated pulling force along pultrusion die for grand fir